Naval Surface Warfare Center
Indian Head Division
Indian Head, MD 20640-5035

IHTR 3217
November 2011

Shock Sensitivity of PBXN-109 When Containing Different RDX Fills Without and With Aging

Harold W. Sandusky

This page intentionally left blank.

REPORT DOCUMENTATION PAGE

Form Approved
OMB No. 0704-0188

1. REPORT DATE *(DD-MM-YYYY)*	2. REPORT TYPE	3. DATES COVERED *(From - To)*
12-09-2010	Summary	2005 - 2010

4. TITLE AND SUBTITLE

Shock Sensitivity of PBXN-109 When Containing Different RDX Fills Without and With Aging

5a. CONTRACT NUMBER

5b. GRANT NUMBER

5c. PROGRAM ELEMENT NUMBER

6. AUTHOR(S)

Harold W. Sandusky

5d. PROJECT NUMBER

5e. TASK NUMBER

5f. WORK UNIT NUMBER

7. PERFORMING ORGANIZATION NAME(S) AND ADDRESS(ES)

Naval Surface Warfare Center, Indian Head Division
Indian Head, MD 20640-5035

8. PERFORMING ORGANIZATION REPORT NUMBER

IHTR 3217

9. SPONSORING/MONITORING AGENCY NAME(S) AND ADDRESS(ES)

OUSD (AT&L)/PSA/LW&M
3090 DEFENSE PENTAGON
ROOM 5C756
WASHINGTON DC 20301-3090

AFRL/RWME
2306 PERIMETER DR
EGLIN AFB, FL 32542

10. SPONSOR/MONITOR'S ACRONYM(S)

11. SPONSOR/MONITOR'S REPORT NUMBER(S)

12. DISTRIBUTION/AVAILABILITY STATEMENT

Approved for public release; distribution is unlimited.

13. SUPPLEMENTARY NOTES

14. ABSTRACT

The influence of different RDX sources on shock reaction and sensitivity was evaluated for a standard explosive in which Class 1 RDX is both the major and only detonable ingredient. Shock reaction in PBXN-109 with seven different RDX fills – Type I, Type II, and reduced sensitivity – from five producers has been studied in three different gap test arrangements. Only the larger tests indicated differences in sensitivity. Dyno Nobel RS-RDX and Royal Ordnance RDX were less sensitive to high velocity detonation (HVD), but exhibited low velocity detonation at a similar threshold as HVD for other fills. After aging for 13 months at 70°C only Dyno Nobel RS-RDX persisted in its insensitivity.

15. SUBJECT TERMS

gap testing, PBXN-109, reduced sensitivity RDX

16. SECURITY CLASSIFICATION OF:			17. LIMITATION OF ABSTRACT	18. NUMBER OF PAGES	19a. NAME OF RESPONSIBLE PERSON
a. REPORT	b. ABSTRACT	c. THIS PAGE			Harold W. Sandusky
Unclassified	Unclassified	Unclassified		48	19b. TELEPHONE NUMBER *(Include area code)* 301.744.2378

This page intentionally left blank.

FOREWORD

Various gap tests were conducted to support the NATO Munitions Safety Information Analysis Center international RS-RDX Round Robin (R4) Program. The objective was to find, develop, and validate methods to distinguish between „normal" and „reduced sensitivity" RDX when formulated into a standard explosive, selected to be PBXN-109. Insensitive high explosives typically have a larger critical diameter (d_c) for propagating detonation, thus the widely used large scale gap test (LSGT) may reflect changes in d_c more so than shock sensitivity. Therefore, sample diameter was doubled in a variation of the expanded large scale gap test (ELSGT) with a reduced sample length to conserve ingredients and aptly named the insensitive munitions advanced development (IMAD) gap test or IMADGT. The effort in the United States was sponsored by the Office of the Under Secretary of Defense for Acquisition, Technology & Logistics, Portfolio Systems Acquisition, Land Warfare and Munitions. The Office of Naval Research provided all RDX ingredients through the Combat Safe Insensitive Munitions program. Technical planning and execution were conducted by Ruth M. Doherty, Matthew J. Domoradski, Nicholas McGregor, Lori A. Nock, and Mary H. Sherlock.

Uncertainty in interpreting the IMADGT results for the insensitive explosives resulted in a subsequent study of one standard and one insensitive fill in PBXN-109 that included LSGT, IMADGT and ELSGT samples from the same mixes. Instrumentation on these tests demonstrated a new phenomenon in shock reaction of the insensitive fill and clarified the interpretation of IMADGT results. Furthermore, the ELSGT for the insensitive fill nearly met the criteria for an extremely insensitive detonating substance or Hazard Class/Division 1.6 explosive. This study was funded internally at the Indian Head Division in the Core Program and was conducted by Harold W. Sandusky, Richard H. Granholm, Joshua E. Felts, and Ruth Doherty.

The relatively short samples IMADGT samples permitted casting twice as many from a 5-gallon mix. Remaining samples from the original castings were used in a subsequent aging study. This Air Force sponsored effort under the direction of the Naval Ordnance Safety & Security Activity was executed by Harold Sandusky and Kerry A. Clark.

Approved and released by:

Gerardo I. Pangilinan

Head, Research and Technology Division

This page intentionally left blank.

CONTENTS

Heading *Page*

Forward……..…….. iv
Contents..…… vi
Acronyms and Abbreviations…….……viii
Introduction ……..……. 1
Experimental Arrangements and Techniques ……..…….. 2
Experimental Results ……...……. 8
LSGT Measurements ……..…… 8
ELSGT Measurements Prior to Aging ……..…… 11
IMADGT Measurements Prior to Aging ……..……. 15
Inclusion of IMADGT Measurements with Aging…… 19
Discussion…….23
Summary and Conclusions…….. 27
References…….. 28
Appendix A: IMADGT Data…….…… 29

Tables

Table I. Types of Class 1 RDX, Mean Particle Size, and HMX Content.....1
Table II. Mix Numbers for All Acceptors. 8
Table III. LSGT Data. 8
Table IV. ELSGT Data.....12
Table V. IMADGT Thresholds for Shock Reaction and SDT Prior to and Following Aging 22

Figures

Figure 1. Proportional sizes of LSGT, ELSGT, and IMADGT (with dimensions).…..…….3
Figure 2. Setup of IMADGT in field…….…… 4
Figure 3. Fixture for dent depth measurement: a. fixture base on dent block and b. with indicator mounted to bar that slides across fixture base to find greatest depth. 5
Figure 4. Comparison of ELSGT calibration with scaled LSGT calibration. 6
Figure 5. Shorting probes on outside of acceptor tubes with gap attached: a. SWs bridging space between two pieces of tape on IMADGT tube; b. SPs in plastic block on ELSGT tube.....7
Figure 6. Comparison of LSGT GO/NOGO data for replicated PBXN-109 mixes with Dyno Nobel RS-RDX and Type II RDX.....9
Figure 7. LSGT witness plates and tube fragments from PBXN-109 filled with Dyno RS-RDX. 9
Figure 8. Probe responses from LSGTs on PBXN-109 filled with Dyno Nobel RS-RDX.....10
Figure 9. LSGT witness plates and tube fragments from PBXN-109 filled with Dyno Nobel Type II RDX.....10
Figure 10. Probe responses from LSGTs on PBXN-109 filled with Dyno Nobel Type II RDX. 11
Figure 11. Comparison of ELSGT GO/NOGO data for PBXN-109 mixes filled with Dyno Nobel RS-RDX and Type II RDX.....12
Figure 12. Probe responses from ELSGTs and One IMADGT on PBXN-109 filled with Dyno Nobel RS-RDX. .13

Figure 13. SG and SP responses near center of ELSGT acceptor containing PBXN-109 filled with Dyno Nobel RS-RDX and subjected to a donor shock attenuated by a 73.63-mm gap. 14
Figure 14. ELSGT acceptor tube fragments (gap end shown to the left) for PBXN-109 filled with Dyno Nobel RS-RDX and subjected to a donor shock attenuated by an 81.27-mm gap. 14
Figure 15. Probe responses from ELSGTs on PBXN-109 filled with Dyno Nobel Type II RDX. 15
Figure 16. IMADGT acceptor tubes recovered after weak shock reaction from PBXN-109 filled with Dyno Nobel RS-RDX. 16
Figure 17. Acceptor tube fragments (gap end shown to the left) and 6.38-mm deep dent in witness block from IMADGT with 88.82-mm gap for PBXN-109 containing Dyno RS-RDX. 17
Figure 18. Witness block dents of 8.23-mm (left) and 10.99-mm (right) in IMADGTs with 70.08- and 68.40-mm gaps, respectively, for PBXN-109 containing Dyno Nobel RS-RDX. 17
Figure 19. Witness block dents of 13.74-mm (left) and 16.90-mm (right) in IMADGTs with 64.06- and 2.54-mm gaps, respectively, for PBXN-109 containing Dyno Nobel RS-RDX. 17
Figure 20. IMADGT data from PBXN-109 with six RDX fills. 18
Figure 21. IMADGT and ELSGT data for PBXN-109 filled with Dyno Nobel RS-RDX. 19
Figure 22. IMADGT and ELSGT data for PBXN-109 filled with Dyno Nobel Type II RDX. 19
Figure 23. IMADGT data for PBXN-109 filled with Eurenco I-RDX. 20
Figure 24. IMADGT data for PBXN-109 filled with Eurenco MI-RDX. 20
Figure 25. IMADGT data for PBXN-109 filled with RO Type I RDX. 21
Figure 26. IMADGT data for PBXN-109 filled with OSI Type II RDX. 21
Figure 27. Effect of Mean Particle Size on P_i for Two Sizes of Gap Tests. 24
Figure 28. Particle Size Distribution for Various Lots of RDX. 24
Figure 29. Reduction of Shock Diameter in Gap Test Donor by Lateral Rarefactions. 25

ACRONYMS AND ABBREVIATIONS

ADI	Australian Defence Industries
AWG	American wire gage
D	Detonation velocity
d_c	Critical diameter for detonation
EIDS	Extremely insensitive detonating substance
ELSGT	Expanded large scale gap test
Eurenco	European Energetics Cooperation
GPa	Gigapascal
HMX	Cylcotetramethylene tetranitramine
HVD	High velocity detonation
IHE	Insensitive high explosive
IP	Ionization pin
IRX	Eurenco insensitive RDX
IMADGT	Insensitive munitions advanced development gap test
LSGT	Large scale gap test
LVD	Low velocity detonation
MI-RDX	Eurenco medium sensitivity RDX
NOL	Naval Ordnance Laboratory
OSI	Ordnance Systems Inc.
P_G	Shock pressure at acceptor end of gap
P_i	Critical shock pressure for SDT
PVC	Polyvinyl chloride
PMMA	Polymethyl methacrylate
RDX	Cylcotrimethylene trinitramine
RISI	Teledyne RISI Inc.
RO	Royal Ordnance
RS-RDX	Reduced sensitivity RDX
SDT	Shock-to-detonation transition
SG	Strain gage
SP	Self-shorting pin
SW	Self-shorting wire
U	Front velocity
x_D	Run distance-to-detonation
δ_{mean}	Mean particle size
ε	Circumferential strain
τ	Shock duration

This page intentionally left blank.

INTRODUCTION

Shock sensitivity of many of the available types of RDX was evaluated in a standard formulation – PBXN-109, which contains Class 1 RDX and aluminum in an inert binder. The seven types of Class 1 RDX are listed in Table 1, along with their lot numbers, Microtrac measurements of mean particle size (δ_{mean}),[1] and HPLC measurements of HMX content[2]. Small-scale safety data are also reported in reference 2.

Table I. Types of Class 1 RDX, Mean Particle Size, and HMX Content

Manufacturer	Type	Lot No.	δ_{mean} (μm)	HMX (%)
Australian Defence Industries (ADI)	Grade A	17211A	215	0.02
Dyno Nobel	RS-RDX	DDP03K001-002	249	0.82
Dyno Nobel	Type II	DDP04L001-002	233	8.55
European Energetics Cooperation (Eurenco)	I-RDX	4904S04	210	0.02
Eurenco	MI-RDX	4902S04	151	0.03
Ordnance Systems Inc. (OSI)	Type II	BAE04M017-039	197	7.36
Royal Ordnance Defence (RO)	Type I	6575	210	0.19

Threshold of shock-to-detonation transition (SDT) is often determined by varying the separation between a donor explosive and the sample, thus the term gap tests. Traditional high explosives are evaluated in the well-known NOL large scale gap test (LSGT). The encased, 36.5-mm diameter sample exceeds the critical diameter (d_c) for steady detonation in many explosives; however, shock input from the donor is applied over a diameter that is smaller than the sample due to rarefactions in the gap. Because of this reduced diameter for shock input, d_c can become limiting prior to the critical shock pressure for SDT (P_i) in insensitive explosives, such as PBXN-109. SDT can still be achieved, but with a shorter gap to provide a shock input of larger diameter, corresponding to a higher pressure in the gap (P_G). Insensitive explosives can be fairly evaluated at double the size of the LSGT in the expanded large scale gap test (ELSGT). The encased sample in both tests has a length of about four times its diameter even though in an unconfined sample SDT is either attained within one sample diameter or fails due to rarefactions. Assuming this principle also applied to encased samples, its length was reduced to 1.4 times the diameter in a version of the ELSGT referred to as the insensitive munitions advanced development (IMAD) gap test or IMADGT. Since detonation of a short sample is less likely to cleanly punch a witness plate, a block is used to indicate reaction violence. All three tests were used in this study to understand differences in shock sensitivity for the various RDX fills. Even then, it was necessary to instrument some tests to interpret results because the shock initiation mechanism was discovered to be different for RDX with reduced sensitivity.

Shock reaction of PBXN-109 with these RDX fills was initially evaluated[2] in 2005 using the IMADGT (firing 12 of the 24 acceptors cast for each fill) and in 2006 using the LSGT for different mixes. Both tests with ADI Grade A RDX exhibited higher than expected sensitivity and are not reported because of a suspected error in incorporating a different RDX in these mixes. A new mix with ADI Grade A RDX achieved the expected LSGT sensitivity, whose datum is reported. Because there was not a definitive determination of the SDT threshold for two insensitive fills, a follow-on study[3] was begun in 2007 to understand those results. Additional IMADGT acceptors from four of the original mixes were tested near the threshold of producing a dent. Several IMADGTs were also conducted on acceptors filled with plastic to obtain tube deformation and block dent without sample reaction. For a standard and insensitive RDX from the same lots, new mixes were made for LSGTs, ELSGTs, and IMADGTs. The LSGTs and IMADGTs were for verifying previously obtained measurements, and the ELSGTs were for relating IMADGT dent measurements to SDT in the full length of an ELSGT acceptor. All LSGTs and some ELSGTs were fired in a bombproof where instrumentation and fragment recovery provided data about growth of shock reaction and run distance-to-detonation (x_D). Remaining IMADGTs and instrumented ELSGTs for the new mixes were fired in field tests.[4] Several ELSGTs with prompt SDT had witness blocks to determine a maximum dent depth in the IMADGT, and P_i in the ELSGT was related to that in the smaller LSGT. In 2008 and 2009, some acceptors from the original 2005 IMADGT castings were aged for 13 months at a controlled 70°C prior to firing.[5]

EXPERIMENTAL ARRANGEMENTS AND TECHNIQUES

The arrangements for the LSGT[6], ELSGT[7], and IMADGT[8] are reviewed in reference 9 and shown in Figure 1 at proportional sizes, with dimensions on the less familiar IMADGT. Shock input in the IMADGT is from the same 1.56 g/cc pentolite donor and polymethyl methacrylate (PMMA) attenuator gap, both with a diameter of 95.3-mm (3 ¾-inch) diameter, as in the ELSGT. In all tests for this study, the donor was initiated with a RISI RP-80 detonator. The IMADGT acceptor (sample) is confined in the same 73.0-mm (2 7/8-inch) inner diameter, 95.2-mm (3 ¾-inch) outer diameter tube of mild steel in the ELSGT, but acceptor length is reduced from 279.4 (11 inch) to 101.6 mm (4 inch). This reduces the requirement for sample ingredients to 36% of that in the ELSGT, which allows more samples per mix or makes testing at this diameter more feasible during scale-up of a new ingredient. Drawn-over -mandrel tubing was probably used for the acceptors because seamless mechanical tubing of that dimension is often unavailable. (Seamless tubing was not directly specified for the ELSGT acceptor[7] but inferred because of being scaled from the LSGT. The version of the ELSGT used in hazard classification for an extremely insensitive detonating substance (EIDS) does specify[10] seamless tubing.) With a long x_D at the SDT threshold, the remaining length of detonating sample may be insufficient to punch a witness plate, so a dent block is used. The 177.8-mm square by 76.2-mm thick (7-inch square by 3-inch thick) block of mild steel is cold-finished with a hardness of Rockwell B70 to B95. The face of the block for witnessing shock reaction is surface ground to clearly display dents and provide an initially flat surface on which to base dent measurements. A 12.7-mm air gap separates the acceptor and dent block, the same as in the insensitive high explosive (IHE) gap test[9]. Several ELSGTs with prompt initiation to assure steady detonation over several sample diameters had this witness arrangement to obtain a maximum dent depth in IMADGTs.

The setup for an IMADGT in the field is shown in Figure 2, with a larger steel plate over the soil to enhance stability. In bombproof tests, another witness block and a 25.4-mm (1-inch) thick polyethylene plate separated the IMADGT from the steel and concrete floor. Since all components above the witness block are the same diameter, their alignment is maintained by wraps of tape as illustrated in Figure 2.

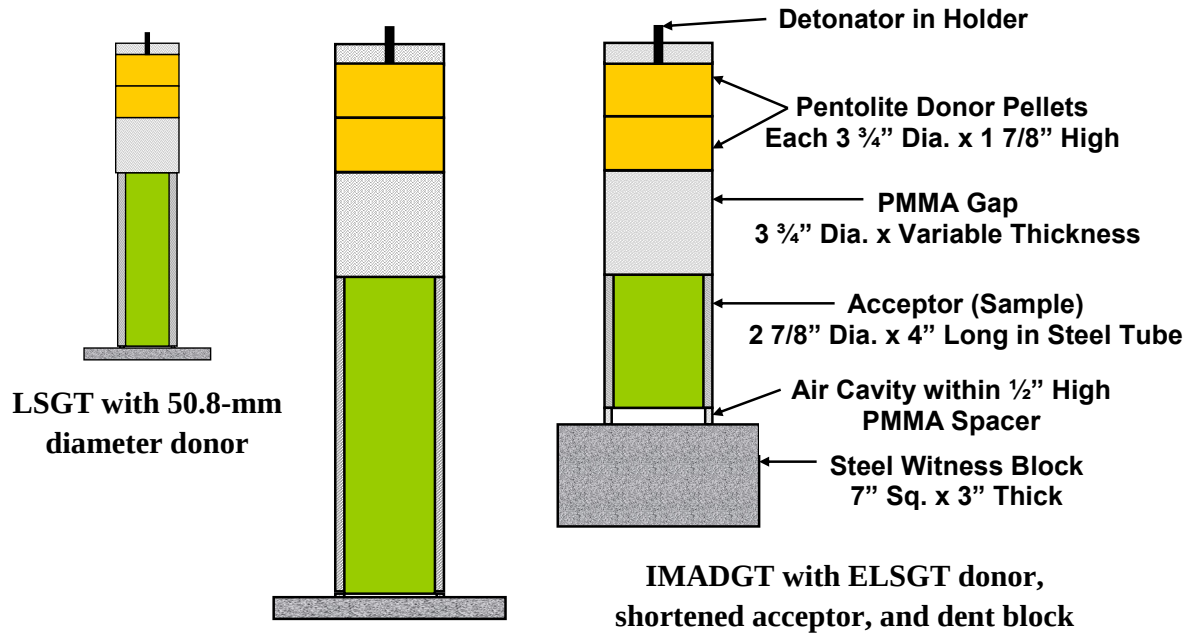

Figure 1. Proportional sizes of LSGT, ELSGT, and IMADGT (with dimensions)

Figure 2. Setup of IMADGT in field

Witness dents ranged from nothing to 15-mm deep and, as will be shown, were useful for distinguishing different levels of shock reaction. Several methods were used to measure dent depth. In the 2005 field tests, each block was stabilized and approximately leveled on a surface plate with the aid of a plastic ring under the block. (The plastic ring was necessary because blocks with deep dents would rock from the opposite surface or bottom being bulged out.) Measurements on the dented surface were obtained by a dial indicator on a magnetic base. Reference measurements were made near the four corners at 12.7 mm (1/2 inch) from each edge and averaged. Six measurements were made near the deepest part of the depression. The greatest depth with respect to the reference is the reported value. It was somewhat cumbersome to find the deepest dent and the corners are slightly raised from bowing of blocks with a bulged bottom. At the bombproof, a dented block was leveled on a milling machine bed using as references the midpoint of each edge, which is less affected than the corners of bulged blocks. Depth measurements were made while translating the block under an indicator secured in the spindle. The deepest dent was readily attained, but only after a time consuming process for leveling the block. In the later tests, measurements were made with a fixture shown in Figure 3. A base rested via set screws onto the midpoint of each edge and had an opening over the central region of the block. An indicator was mounted to a bar that slid across that opening to find the greatest depth, which was not always in the center of the depression. Accuracy was verified for blocks previously measured on the milling machine.

a. b.

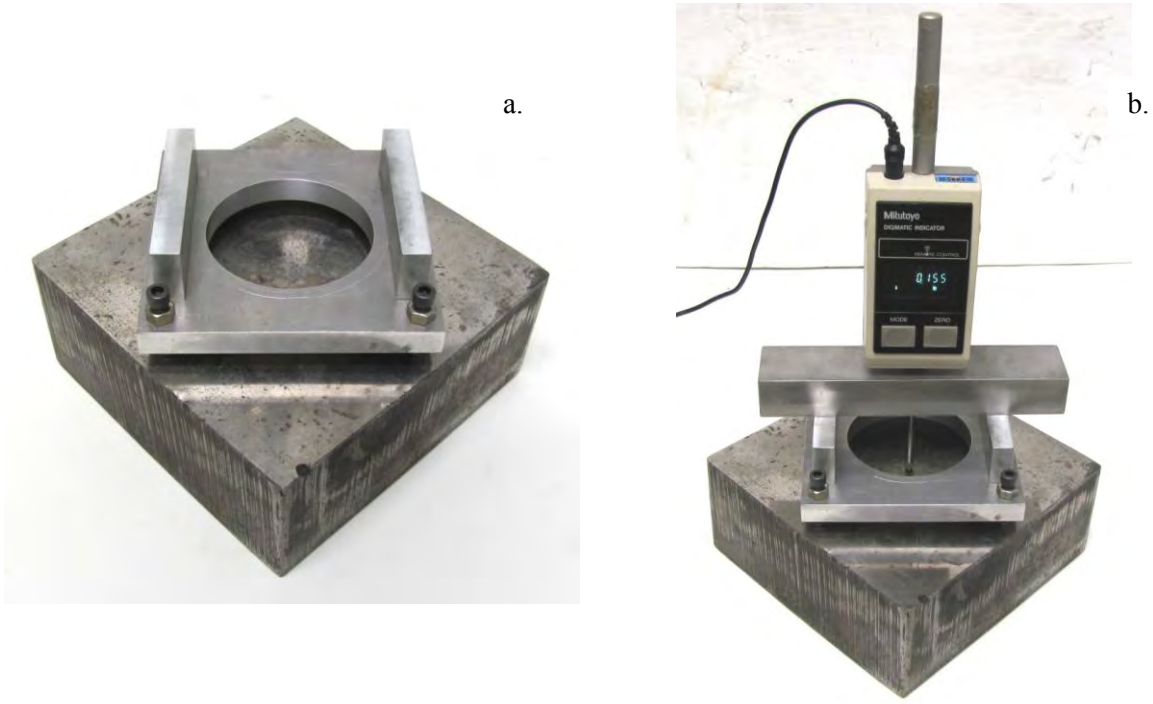

Figure 3. Fixture for dent depth measurement: a. fixture base on dent block and b. with indicator mounted to bar that slides across fixture base to find greatest depth

Some IMADGT and ELSGT gaps for PBXN-109 tests exceed the 102-mm maximum for the P_G calibration. The experimental calibration of ELSGT donor corresponds to that for the LSGT with gap thickness increased by 1.75 times instead of the 1.875 ratio of donor dimensions,[9] as shown in Figure 4. (Sutherland[10] recently provided some insight as to why P_G from these 1.56 g/cc pentolite donors doesn't scale.) This extends the ELSGT calibration to gaps of 236 mm (9.30 inches), which is in excess of the largest gaps in this study. For consistency, all reported values of P_G for IMADGTs and ELSGTs are scaled from the LSGT calibration equations for a pentolite donor on page 10 of reference 6.

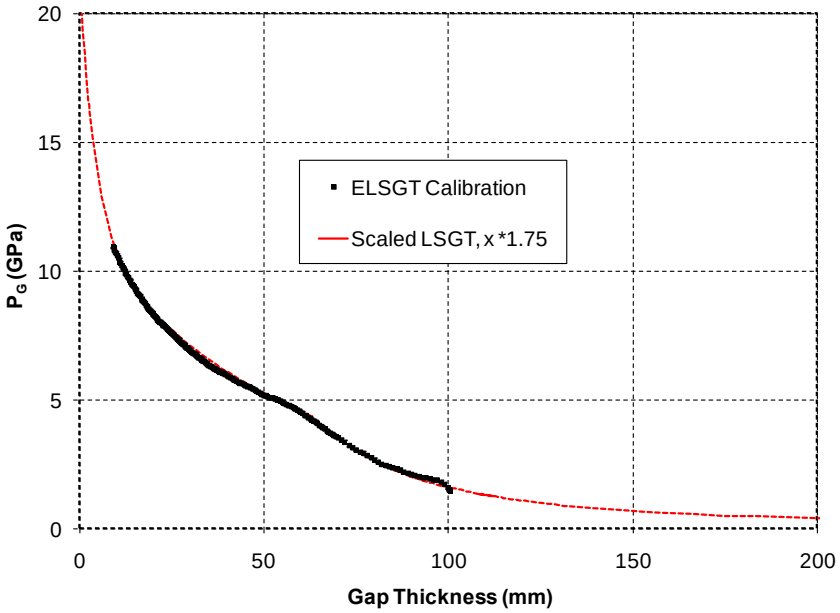

Figure 4. Comparison of ELSGT calibration with scaled LSGT calibration

For the follow-on study beginning in 2007, the position of shock/reaction fronts was measured with three types of probes, but all were basically switches that shorted capacitive discharge circuits. The simplest type was a shorting wire (SW) on the outer wall of the acceptor tube. The insulation is removed from one end of a solid 22 AWG wire that is taped down circumferentially over a piece of Teflon film used for sealing pipe threads. Any rapid expansion of the tube wall causes the wire to press through the Teflon film and contact the grounded tube. A variation, which was equally successful, is shown in Figure 5a, where the SWs bridged a small 1.3-mm (0.05-inch) gap between two pieces of white tape along the length of the tube. Another type of probe for the outside of the tube wall was low-pressure self-shorting pins (SPs). Dynasen model CA-1042 SPs were bonded in a plastic block that is taped to the tube, as shown in Figure 5b. The SP locations are more precise than for SWs and much of the preparation occurs before mounting on the tube. In additional to the external probes, some measurements were made with ionization pins (IPs). Dynasen model CA-1040 IPs were inserted into the sample 6.3 mm (0.25 inch) past the inner wall of the tube. This required having the probe holes drilled into tubes and then filling those holes with a sealant prior to casting the explosive. After the explosive had cured, the sealant was removed and the hole extended into the sample with a drill in a pin vise. This is a tedious process because the drill has to be removed after only several rotations to clean the flutes before continuing.

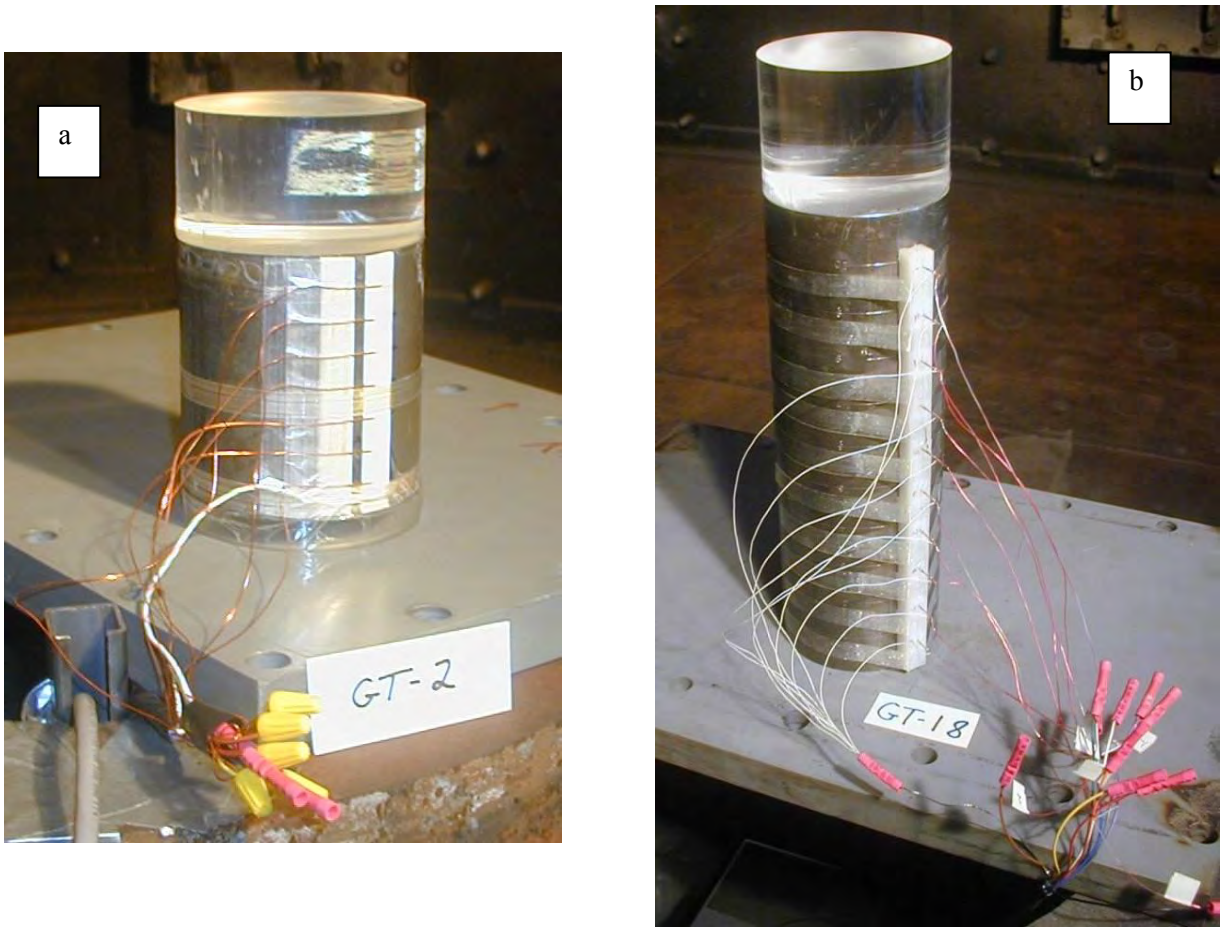

Figure 5. Shorting probes on outside of acceptor tubes with gap attached: a. SWs bridging space between two pieces of tape on IMADGT tube; b. SPs in plastic block on ELSGT tube

Several tests had a strain gage (SG) circumferentially-mounted on the outer tube wall to observe pressure buildup from the sample at that location. Measurement of up to 10% strain (ε) was achieved using high elongation gages of annealed constantan bonded with a urethane adhesive that does not require temperature curing as does an epoxy of similar elongation. This was necessary because the tubes were already filled with the PBXN-109. SGs with low resistance (120 Ω), thus wider segments in their grid pattern, better survived the initially rapid tube expansion from shock arrival. SGs were connected to a Wheatstone bridge with constant supply voltage whose output was directly recorded on an oscilloscope without an intermediate amplifier.

The outer wall of each acceptor tube was marked with permanent ink or stamped every inch from an end at four places equally spaced on the circumference. Even with tube fragments impacting a steel barbette in the firing chamber, enough markings were still visible to determine where tube fragments originated from.

EXPERIMENTAL RESULTS

Table II lists the last three digits of the mix number for each type of acceptor and the year it was processed, not necessarily when the acceptors were tested. There was no indication that replicated IMADGT and LSGT mixes with Dyno Nobel RS-RDX and Type II RDX provided different results. The following tables of data for the various tests reference those mix numbers.

Table II. Mix Numbers for All Acceptors

RDX	2005 IMADGT Mix No.	2006 LSGT Mix No.	2007 LSGT, ELSGT, IMADGT Mix No.
ADI Grade A		320	
Dyno Nobel RS-RDX	307	099	225
Dyno Nobel Type II RDX	308	100	226
Eurenco I-RDX	302	098	
Eurenco MI-RDX	301	128	
OSI Type II	306	127	
RO Type I	300	126	

LSGT Measurements

LSGT data are summarized in Table III, with only the critical gap provided for the 2006 test series[2] on twelve acceptors for each mix. GO/NOGO determinations from the two 2007 mixes are consistent (Figure 6) with the critical gaps from earlier mixes. The ~10-mm difference in critical gap thickness between mixes with Dyno Nobel RS-RDX and Type II RDX corresponds to ~1.5 GPa change in P_G.

Table III. LSGT Data

RDX	Mix No.	Gap (in)	Gap (mm)	P_G (GPa)	GO/NOGO*
ADI Grade A	320	1.135	28.83	5.22	Critical
Dyno Nobel RS-RDX	099	1.130	28.70	5.24	Critical
	225	1.097	27.86	5.35	GO
		1.129	28.68	5.24	GO
		1.140	28.96	5.21	NOGO
		1.150	29.21	5.17	NOGO
Dyno Nobel Type II RDX	100	1.505	38.23	3.86	Critical
	226	1.450	36.83	4.16	GO
		1.5025	38.16	3.87	GO
		1.5507	39.39	3.63	NOGO0
		1.6505	41.92	3.18	NOGO
Eurenco I-RDX	098	1.310	33.27	4.66	Critical
Eurenco MI-RDX	128	1.945	49.40	2.21	Critical
OSI Type II	127	1.445	36.70	4.19	Critical
RO Type I	126	1.185	30.10	5.06	Critical

*GO or NOGO designated for individual tests, Critical is for a series of 12 tests

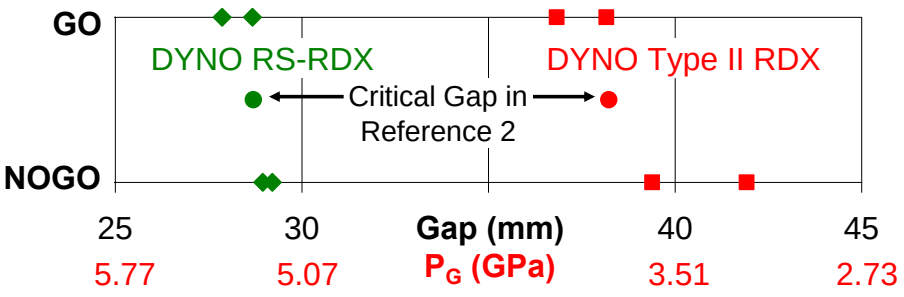

Figure 6. Comparison of LSGT GO/NOGO data for replicated PBXN-109 mixes with Dyno Nobel RS-RDX and Type II RDX

For the 2007 mix with the Dyno RS-RDX fill, photographs of recovered hardware near the critical gap are shown in Figure 7. LSGT witness plates were 228.6-mm (9-inches) square to avoid breakup, as is currently done in testing at this Center, versus the original[6] 101.6-mm (4-inches) square plate. For a 28.68-mm (1.129-inch) gap there was a cleanly punched hole in the witness plate and small tube fragments (not shown) indicative of a GO. For an increase of one card (0.25 mm or 0.01 inch) in gap thickness, there were sizeable tube fragments and a plate with a 6-mm depression, indicative of a NOGO. With another card increase in thickness, there were similar tube fragments but a punched plate with a partially torn hole, indicative of shock reaction but not SDT. IP data for these tests are displayed in Figure 8 along with SP data for another test with a reduced 27.86-mm gap. For this shortest gap with P_G = 5.35 GPa, SDT occurred at ~50 mm into the sample with a detonation velocity (D) of 7.54 mm/μs. The three longer gaps (those with photographs of recovered hardware in Figure 7) had a similar P_G (5.24 to 5.17 GPa) and initial 2.9 mm/μs front velocity (U). For the shorter gap, that front began accelerating after 50 mm and transited at ~100 mm. For the two longer gaps, that 2.9 mm/μs front continued to steadily propagate. Thus, SDT can occur near the far end of the acceptor; and at slightly lower P_G, a steady front at < ½ D can still penetrate the witness plate.

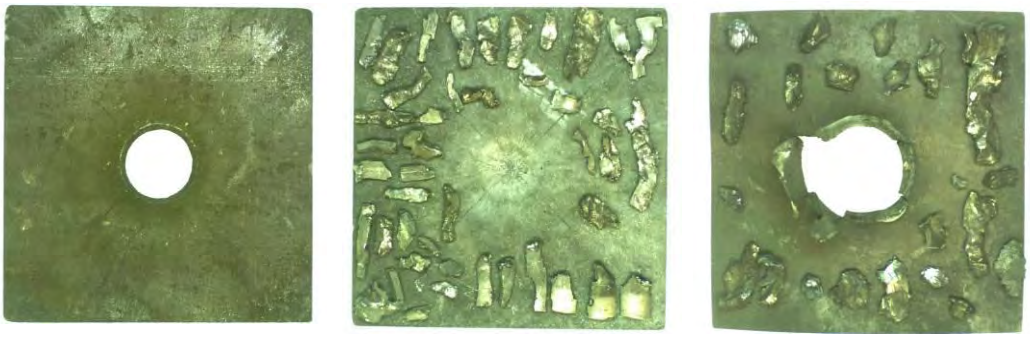

Figure 7. LSGT witness plates and tube fragments from PBXN-109 filled with Dyno RS-RDX

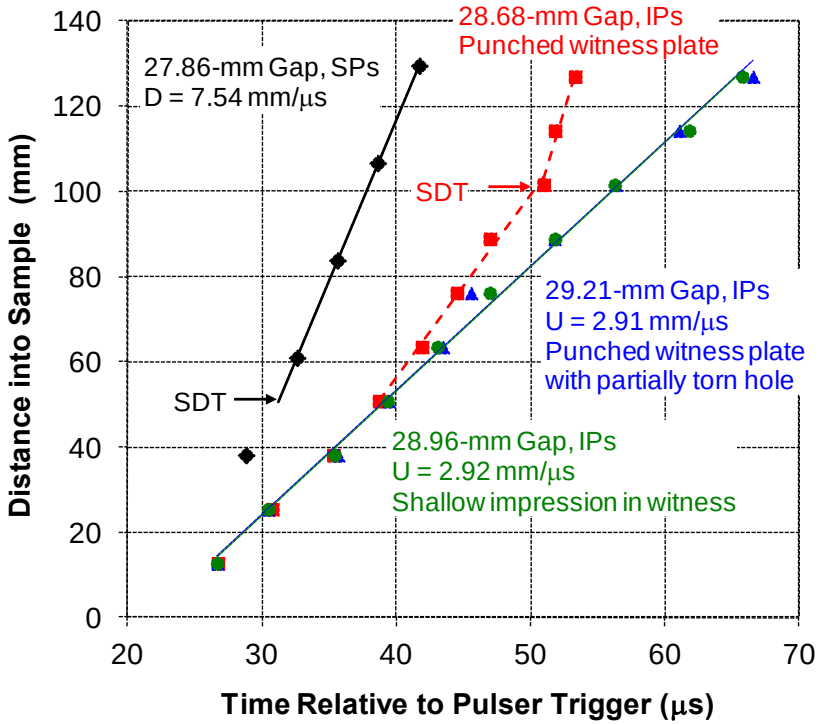

Figure 8. Probe responses from LSGTs on PBXN-109 filled with Dyno Nobel RS-RDX

For the 2007 mix with the Dyno Type II RDX fill, photographs in Figure 9 show greater differences in tube fragmentation because of the wider range of gaps than for tests in Figure 7. There was a cleanly punched hole (gray band in hole is a ruler) and small tube fragments (not shown) for the 38.16-mm gap, large tube fragments and a 13-mm deep impression in the witness plate for the 39.39-mm gap, and split pieces of tube and a shallow impression in the plate for the 41.92-mm gap. These differences are reflected by the pin data in Figure 10. There were no probe data for the 38.16-mm gap, but SDT occurred promptly with $x_D < 40$ mm for a 5-card shorter, 36.83-mm gap. The 8.19 mm/μs detonation velocity is higher than in other tests. There was no acceleration of the initial reaction front for the longer gaps. The 39.39-mm gap induced a steady 2.97 mm/μs front versus an initial 2.78 mm/μs front that began failing after 64 mm for the 41.92-mm gap.

Figure 9. LSGT witness plates and tube fragments from PBXN-109 filled with Dyno Nobel Type II RDX

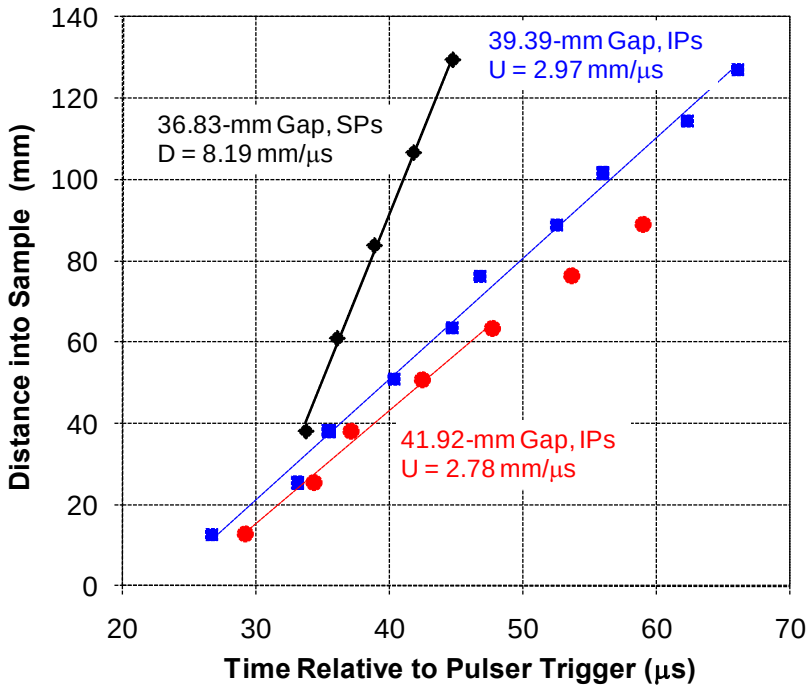

Figure 10. Probe responses from LSGTs on PBXN-109 filled with Dyno Nobel Type II RDX

ELSGT Measurements

ELSGT data for the mixes with Dyno Nobel RS-RDX and Type II RDX are summarized in Table IV. A test with prompt detonation (short gap) and a witness block replacing the usual plate was conducted for each mix to determine the maximum dent depth that could be expected in the IMADGT. As will be shown, plates are not always a definitive witness for high velocity detonation (HVD), so there is the future possibility of using dent blocks for ELSGTs. Each test in Table IV had probes for verifying detonation except for one on the Dyno Nobel Type II RDX mix with a 103.25-mm gap, which only had a SG. In this table, a GO requires a punched plate (or deep dent) and a probe measurement of HVD. Three tests for the RS-RDX mix had cleanly punched witness plates but with U < ½ D, which is low velocity detonation (LVD). GO/NOGO determinations from Table IV are displayed in Figure 11. The test on the Type II RDX fill at a gap of 103.25 mm that did not have probe data to accompany the punched witness plate is distinguished by plotting this datum between a GO and NOGO. The critical gap for the RS-RDX fill is very near the maximum 70 mm for an EIDS.

Table IV. ELSGT Data

RDX	Mix No.	Gap (in)	Gap (mm)	P_G (GPa)	GO/NOGO*	Comments
Dyno Nobel RS-RDX	225	2.449	62.20	4.40	GO	Witness block with 16.6-mm dent
		2.450	62.23	4.40	GO	
		2.749	69.82	3.53	GO	
		2.798	71.07	3.40	GO	
		2.847	72.31	3.28	NOGO	Punched plate
		2.899	73.63	3.16	NOGO	Punched plate
		3.1995	81.27	2.54	NOGO	Punched plate
		3.6465	92.62	1.89	NOGO	Slight plate dent
Dyno Nobel Type II RDX	226	3.600	91.44	1.95	GO	
		3.700	93.98	1.84	GO	Witness block with 15.2-mm dent
		3.8005	96.53	1.73	GO	
		3.902	99.11	1.64	GO	
		4.000	101.60	1.55	GO	
		4.0005	101.61	1.55	NOGO	Slight plate dent
		4.065	103.25	1.50	Probable GO	No probes for verifying detonation
		4.202	106.73	1.40	NOGO	No plate damage

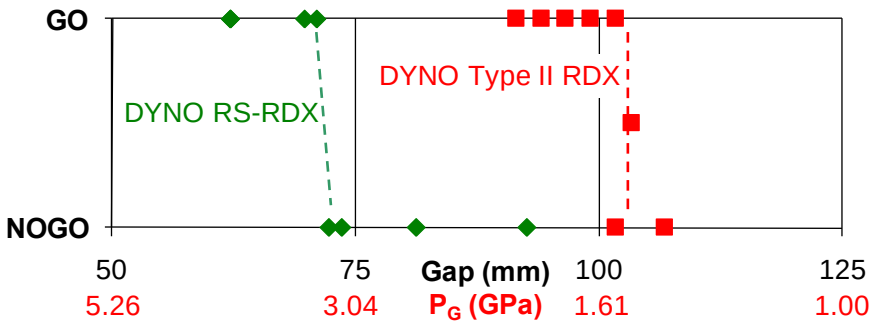

Figure 11. Comparison of ELSGT GO/NOGO data for PBXN-109 mixes filled with Dyno Nobel RS-RDX and Type II RDX

For the Dyno RS-RDX fill, probe data from eight ELSGTs cast in 2007 and one IMADGT cast in 2005 are plotted in Figure 12. The large range in gap thickness shows the initial U decreasing with longer gaps. For the shortest, 62-mm gaps, prompt SDT occurred in <5 μs after shock entry into the acceptor (~40 μs from initiation of the detonator) and at <25 mm from the gap. With 70- and 71-mm gaps, SDT occurred after a delay of ~50 μs at

~200 mm, near the end of the acceptor as also observed in the LSGT. For longer gaps, relatively steady fronts propagated the length of the acceptor, being sustained by weak shock reaction. For gaps between 72 and 81 mm, reaction fronts with U >3.18 mm/μs (somewhat greater than the 1.75 mm/μs sound velocity but < ½ D) cleanly punched the witness plate. The test with a 73.63-mm gap also had a SG at 127 mm, whose signal is displayed in Figure 13 along with responses of nearby SPs. Beginning at ~75 μs when the front reached the SG position, there was a linear rise to 5% ε at 92 μs, an indication of only weak shock reaction. Acceptor fragments are a better indication of detonation but only recovered in bombproof tests. The long fragments shown in Figure 14 that were recovered from the witness end of the acceptor in the test with an 81.27-mm gap do not indicate HVD.

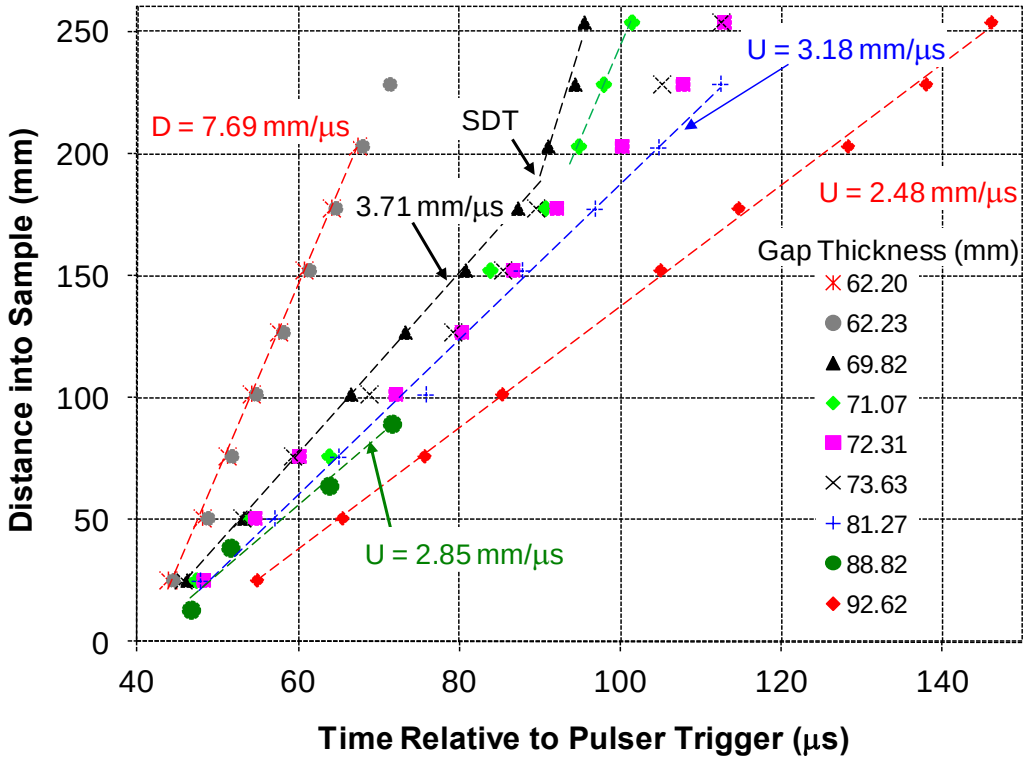

Figure 12. Probe responses from ELSGTs and One IMADGT on PBXN-109 filled with Dyno Nobel RS-RDX

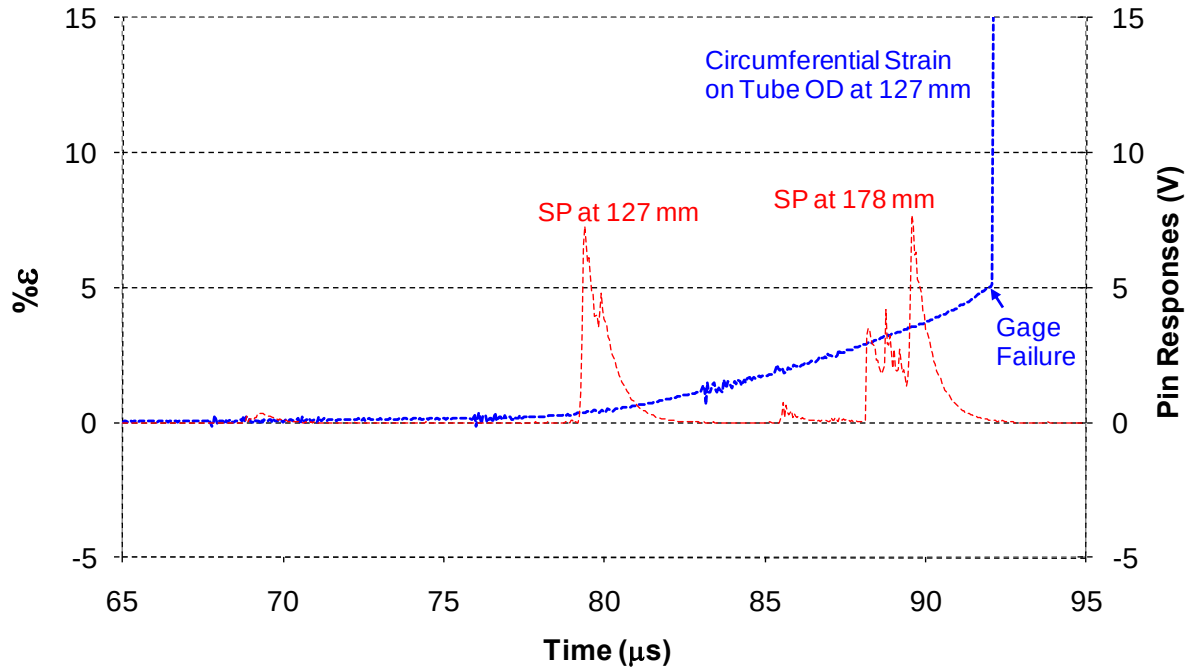

Figure 13. SG and SP responses near center of ELSGT acceptor containing PBXN-109 filled with Dyno Nobel RS-RDX and subjected to a donor shock attenuated by a 73.63-mm gap

Figure 14. ELSGT acceptor tube fragments (gap end shown to the left) for PBXN-109 filled with Dyno Nobel RS-RDX and subjected to a donor shock attenuated by an 81.27-mm gap

For PBXN-109 filled with Dyno Type II RDX, shock reaction either failed or rapidly grew over a narrow range of gaps (Figure 15). SDT occurred at ~60 mm for a 91.4-mm gap and ~90 mm for a 96.5-mm gap. With a 101.6-mm gap, the initial 2.74 mm/μs front accelerated after ~75 mm to SDT in one test but began failing at that distance in another test with most of the explosive recovered along with only a slight depression in the witness plate. For a 106.73-mm gap, no reaction was detected after 50 mm. In an additional test without pins but with a SG at 127 mm, the witness plate was cleanly punched for a 103.25-mm gap. Beginning at ~98 μs, there was a linear rise to 10% ε at 115 μs, indicating a greater delay in reaction acceleration than in the one detonating test with a 101.60-mm gap.

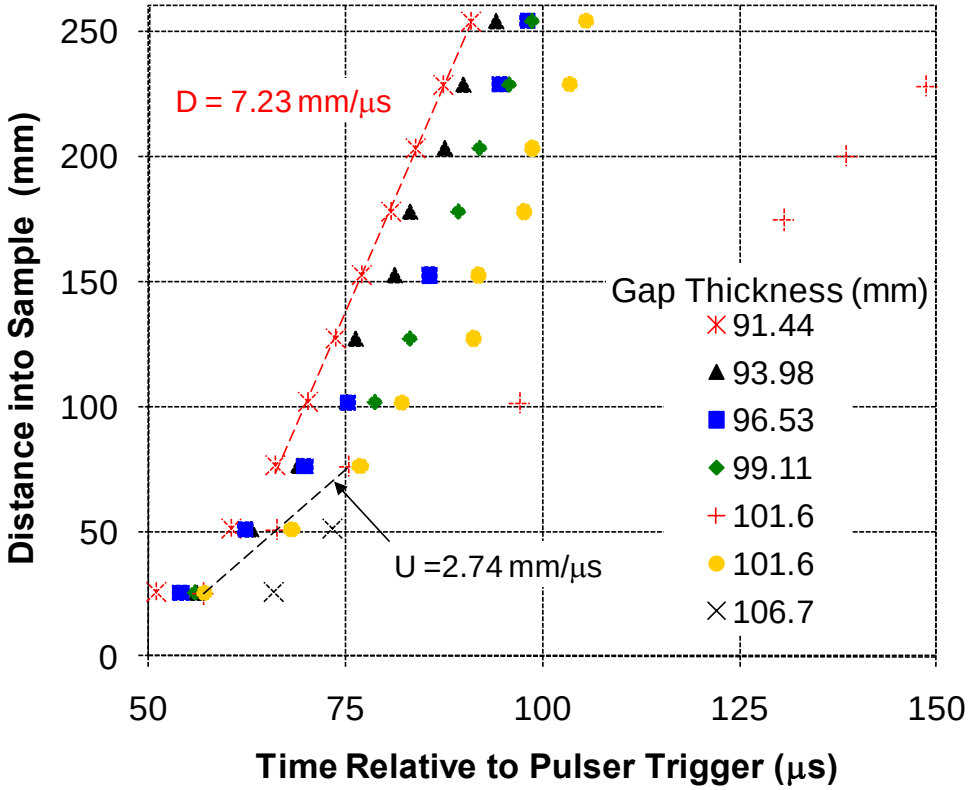

Figure 15. Probe responses from ELSGTs on PBXN-109 filled with Dyno Nobel Type II RDX

IMADGT Measurements Prior to Aging

The shock strength required to expand acceptor tubes and dent witness blocks was assessed in tests with plastic samples that spanned the density of PBXN-109 – polyvinyl chloride (PVC) with a density 1.385 g/cc and Teflon with a density of 2.171 g/cc. With a 101.7-mm gap, which is at the threshold for denting witness blocks with PBXN-109, the gap end of a tube filled with PVC had expanded by 1.9% without denting the block. With a 50.8-mm gap, the gap end of tubes filled with PVC and Teflon had expanded 33.3% and 34.9%, respectively; the witness ends had expanded <0.5%; and dent depth in the blocks was <0.1 mm. Therefore, the tube breakup and witness block dents observed with PBXN-109 samples were from shock reaction.

Recovered hardware from bombproof tests for the Dyno Nobel RS-RDX fill illustrates the progression of damage with increasing P_G. Figure 16 shows minimal shock reaction for a 109.65-mm gap (gap end expanded by about twice that for a plastic sample) that decayed toward the witness end, but somewhat increased reaction with growth towards the witness end for a 104.62-mm gap that produced a 0.05-mm dimple in the block. For a 101.54-mm gap, the acceptor tube split but the witness dent was still only 0.13 mm. For an 88.82-mm gap, the tube fragmented with pieces from the gap end smaller than from the witness end and some even smaller pieces from the center, as shown in Figure 17 which includes a 6" ruler. While this is vigorous shock reaction, there was no acceleration for attaining SDT. The 6.38-mm deep dent shown in Figure 17 had a smooth descent to a uniform bottom, which is typical when near the threshold of producing a dent. For the 8.23- and 10.99-mm deep dents photographed in Figure 18, there is first a ring of metal flow at the bottom edge of the depression and then increased damaged there. For the 13.74- and 16.90-mm deep dents photographed in Figure 19, the bottom of the dent remains flat while the transition from the surface of the blocks becomes a steep descent with a raised edge and then a crater with metal pushed outward. The maximum 16.90-mm dent depth was attained with the minimum, 2.54-mm gap thickness and is essentially the same as that in an ELSGT with prompt detonation (Table IV).

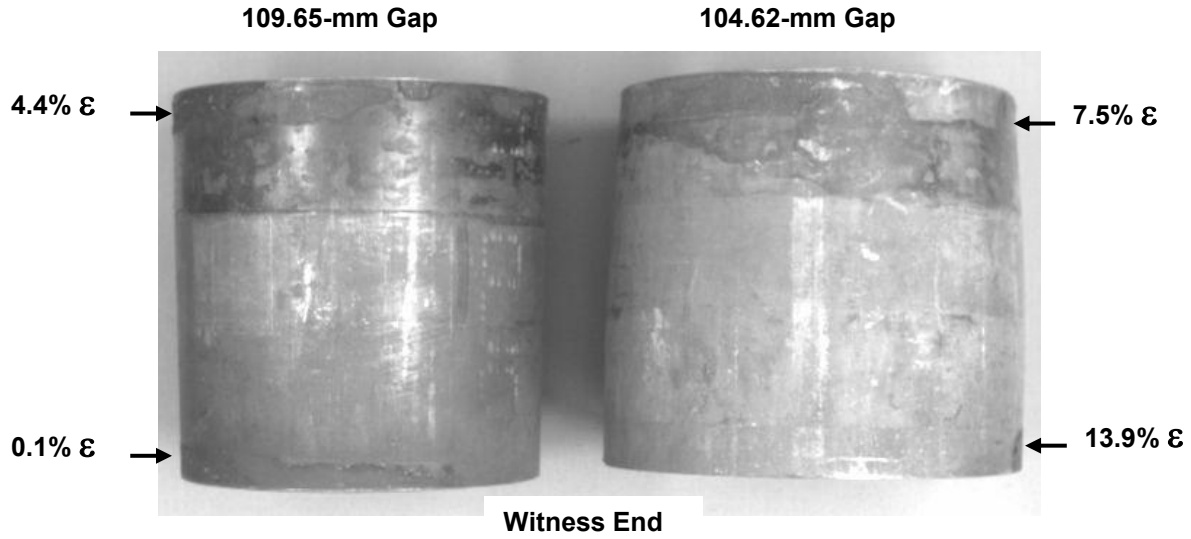

Figure 16. IMADGT acceptor tubes recovered after weak shock from PBXN-109 filled with Dyno Nobel RS-RDX

Figure 17. Acceptor tube fragments (gap end shown to the left) and 6.38-mm deep dent in witness block from IMADGT with 88.82-mm gap for PBXN-109 containing Dyno RS-RDX

Figure 18. Witness block dents of 8.23-mm (left) and 10.99-mm (right) in IMADGTs with 70.08- and 68.40-mm gaps, respectively, for PBXN-109 containing Dyno Nobel RS-RDX

Figure 19. Witness block dents of 13.74-mm (left) and 16.90-mm (right) in IMADGTs with 64.06- and 2.54-mm gaps, respectively, for PBXN-109 containing Dyno Nobel RS-RDX

All IMADGT data are tabulated in Appendix A and plotted together in Figure 20. (The next section contains an individual plot for each fill.) Dent measurements were unaffected by test date (listed), test personnel and location, and even different mixes for the two Dyno Nobel fills. Not shown in Figure 20 are tests conducted with gaps >115 mm, which had no dent; and tests with gaps of 2.5 mm, which had a consistent but ~1.5-mm deeper dent than for a 50.8-mm gap. There was a distinct change from no witness block dent to a depth of >5 mm at what is referred to as the onset of sustained shock reaction. This occurred between gaps of 100 and 112 mm for all fills (100-mm gap for Dyno Nobel RS-RDX, 105-mm gap for RO Type I RDX, ~111-mm gap for Eurenco MI-RDX and OSI RDX, and ~112-mm gap for Dyno Nobel Type II RDX and Eurenco I-RDX). Since P_G changes slowly for long gaps (Figure 4, which is also evident from values on the major divisions in Figure 20), the onset of sustained shock reaction in PBXN-109 is ~1.25 GPa for all sources of RDX. At slightly longer gaps there was tube deformation from weak shock reaction without denting the witness block, as shown for the Dyno Nobel RS-RDX fill in Figure 16.

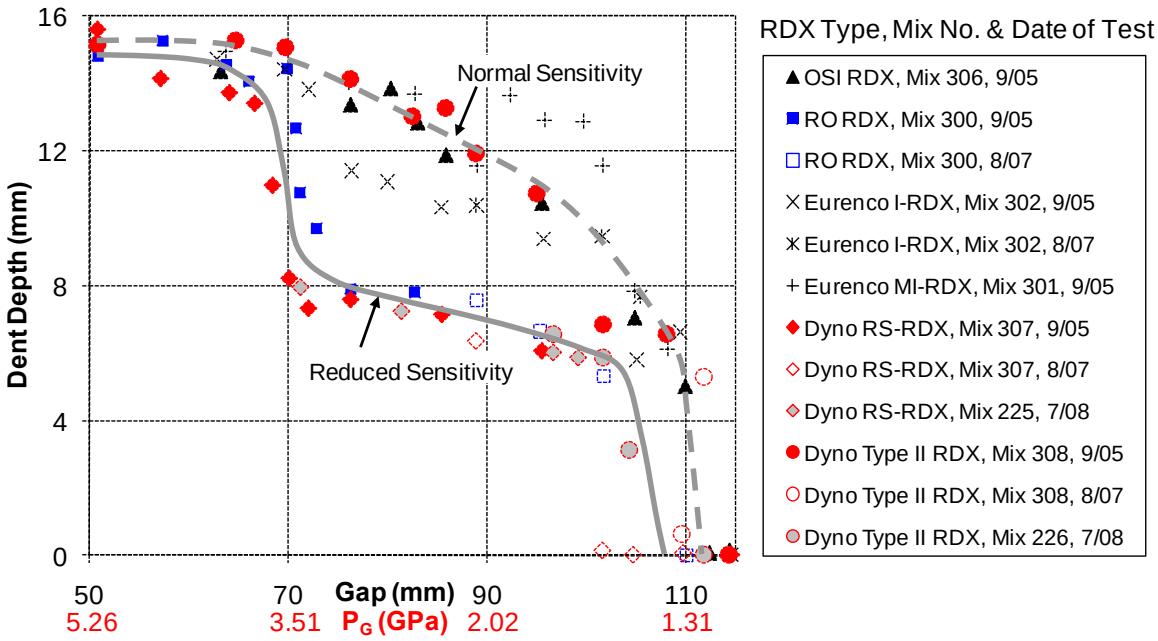

Figure 20. IMADGT data from PBXN-109 with six RDX fills

Following the appearance of dents, reduced gaps produced deeper dents. The one exception was for the Dyno Nobel Type II RDX fill, which had two lesser dents after first attaining a 5.3-mm deep dent at a 111.71-mm gap with P_G = 1.27 GPa. Four fills – OSI RDX, Eurenco I-RDX, Eurenco MI-RDX, and Dyno Nobel Type II RDX – exhibited normal sensitivity with rapidly increasing dent depth indicative of imminent SDT, shown as the dashed gray line in Figure 20. The other two fills – RO RDX and Dyno Nobel RS-RDX – had reduced sensitivity with a gradual increase in dent depth until gaps of ~70 mm, which is a factor of two increase in P_G from the onset of sustained shock reaction, shown as the solid gray line. It was this unusual behavior that required instrumented ELSGTs to relate dent depth measurements to SDT. As gap thickness is further reduced to <60 mm, prompt shock reaction in all fills produced a comparable dent from SDT, probably with a similar x_D.

Inclusion of IMADGT Measurements with Aging

IMADGT dent measurements prior to aging (solid line) and following aging for 13 months at 70°C (dashed line) are related to ELSGT GO/NOGO data for PBXN-109 with Dyno Nobel RS-RDX in Figure 21, while a similar comparison is made for the Dyno Nobel Type II RDX fill in Figure 22. The threshold for shock reaction was unchanged by aging, but the Type II RDX fill again had a reduced dent for a slight increase in P_G above the threshold. A ~8-mm deep dent in the IMADGT corresponded to the critical gap in the ELSGT (72.1 mm for the RS-RDX fill and 103.2 mm for the Type II RDX fill). As noted in Figure 21 and Table IV, three ELSGTs with gaps exceeding critical had punched witness plates without SDT. Each figure also has a dent measurement from one promptly detonating ELSGT with a witness block instead of a plate that compared well with the maximum IMADGT dent depth.

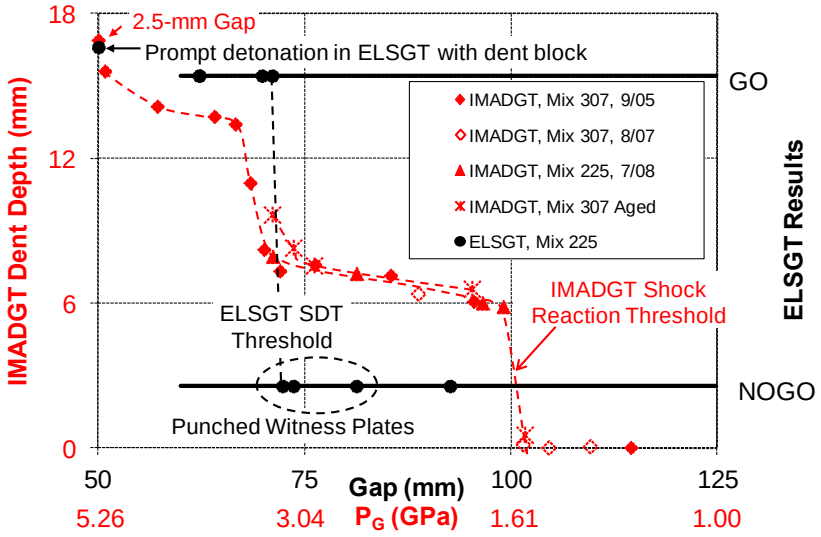

Figure 21. IMADGT and ELSGT data for PBXN-109 filled with Dyno Nobel RS-RDX

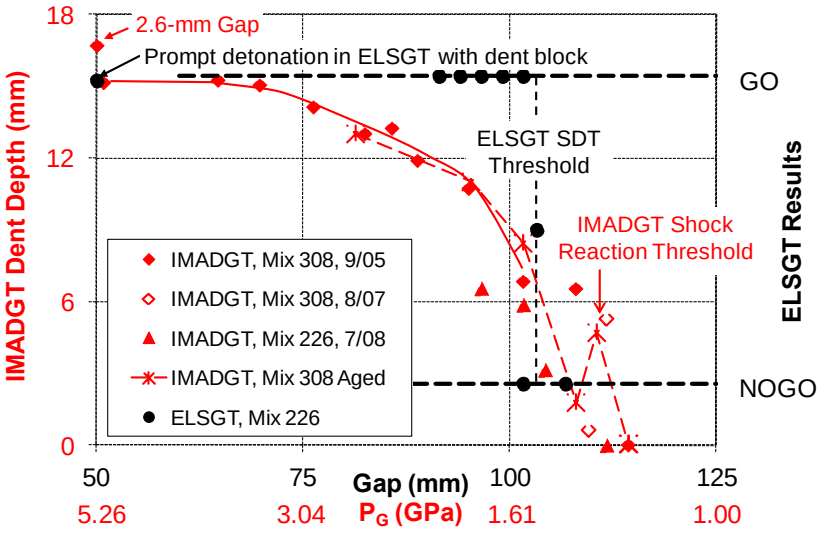

Figure 22. IMADGT and ELSGT data for PBXN-109 filled with Dyno Nobel Type II RDX

IMADGT data for PBXN-109 with Eurenco I-RDX, Eurenco MI-RDX, RO Type I RDX, and OSI Type II RDX are plotted, respectively, in Figures 23-26. Both Eurenco fills have a small increase in sensitivity for the aged acceptors and anomalous responses near the threshold of shock reaction. RO RDX exhibits a small shift in the onset of shock reaction with aging, but significant increases in dent depth for higher shock pressures instead of the gradual increases prior to aging. Thus, the SDT threshold for RO RDX reverts to that for typical, more sensitive fills. OSI RDX has significant decreases in the thresholds of both shock reaction and SDT.

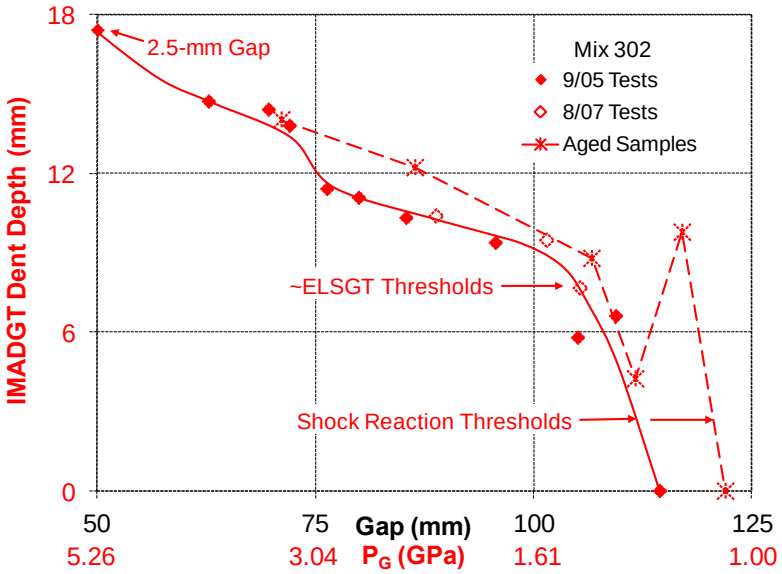

Figure 23. IMADGT data for PBXN-109 filled with Eurenco I-RDX

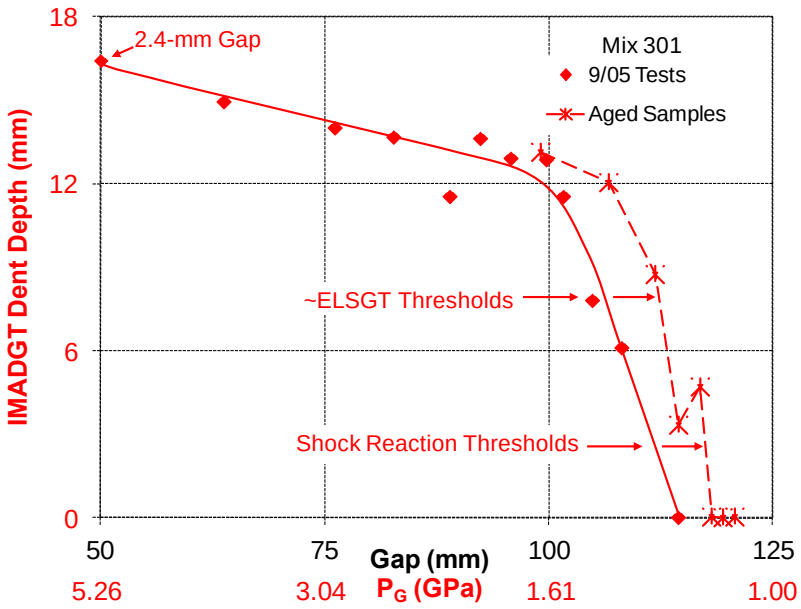

Figure 24. IMADGT data for PBXN-109 filled with Eurenco MI-RDX

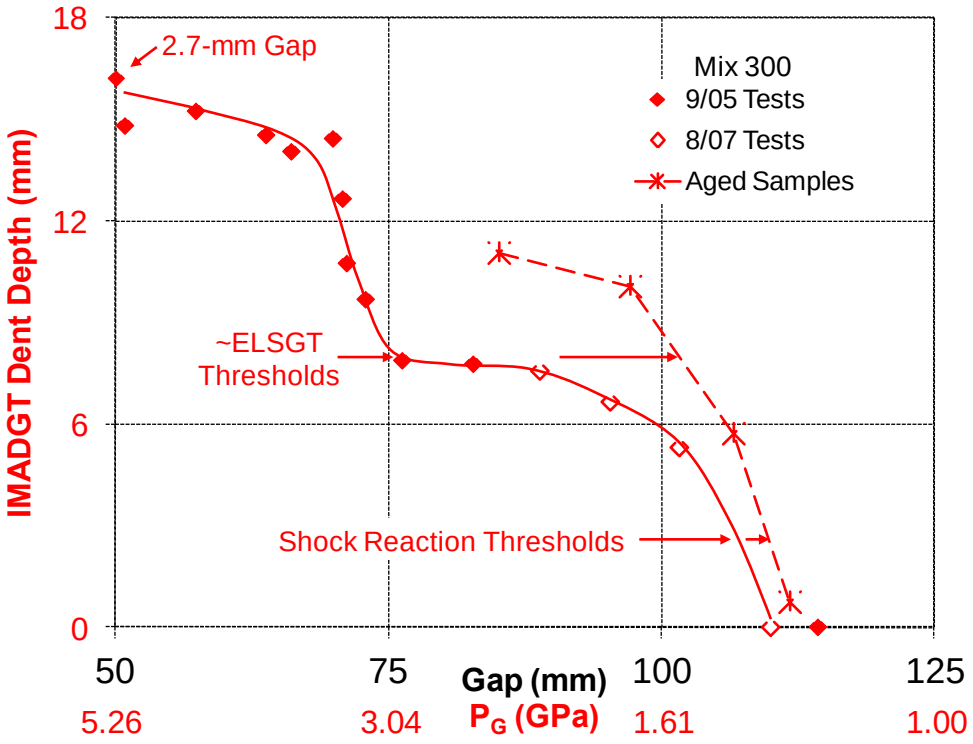

Figure 25. IMADGT data for PBXN-109 filled with RO Type I RDX

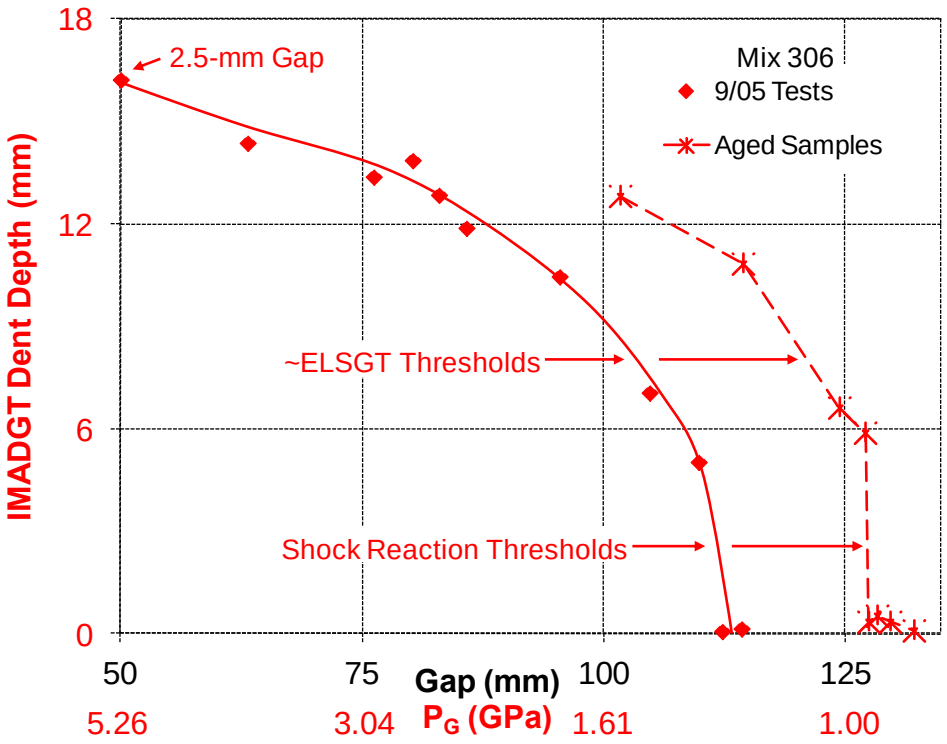

Figure 26. IMADGT data for PBXN-109 filled with OSI Type II RDX

Table V lists thresholds for shock reaction and SDT, the latter estimated to correspond to an 8-mm dent depth in the IMADGT. Unaged data for Dyno Nobel RS-RDX and RO Type I RDX include an additional SDT threshold for LVD at a significantly lower P_G than for HVD. These lower thresholds for LVD and the thresholds for HVD in the other fills are at only slightly higher P_G than the threshold for shock reaction. IMADGT data in Figure 21 suggests that LVD persisted for the aged Dyno Nobel RS-RDX fill, but without verification by probes.

Table V. IMADGT Thresholds for Shock Reaction and SDT Prior to and Following Aging

Fill	Thresholds, P_G (GPa)			
	Shock Reaction		SDT	
	Unaged	Aged	Unaged	Aged
Dyno RS-RDX	1.60	1.65	3.30, 1.64	2.93
Dyno Type II	1.27	1.26	1.62	1.53
Eurenco I-RDX	1.27	1.10	1.44	1.37
Eurenco MI-RDX	1.29	1.14	1.45	1.25
RO Type I	1.43	1.40	2.93, 1.55	1.53
OSI Type II	1.29	0.96	1.51	1.05

Rather than fire all aged IMADGT acceptors, one each with Eurenco MI-RDX, RO Type I RDX, and OSI Type II RDX fills were cored out for analysis.[5] Differential Scanning Calorimetry tests indicated a decrease in the onset temperature for reaction in the fills with Eurenco MI-RDX and RO RDX. The drop-weight impact sensitivity for aged samples remained low with the RO RDX fill being slightly more sensitive. Scanning Electron Microscopy showed isolated browning of RO RDX crystals, significant browning in OSI RDX, but none in Eurenco MI-RDX. The browning commences at isolated spots within crystals and is currently being studied with assistance from the IMAD Program and BAE Holston Inc.

DISCUSSION

IMADGT and ELSGT data for fills with reduced and typical RDX sensitivity reveal different shock reaction mechanisms. For Dyno Nobel Type II RDX, which has typical sensitivity, a modest increase in shock pressure beyond the reaction threshold produced a deeper dent in the IMADGT witness block and an accelerating front near the gap in the ELSGT that transited to HVD. This is characteristic of shock reaction models in which reaction rate increases with pressure to a power greater than one. For the insensitive Dyno Nobel RS-RDX fill, an increase in shock pressure just beyond the reaction threshold did not significantly increase the IMADGT dent depth and a steady front propagated at less than half the velocity for HVD in the longer ELSGT acceptor. Such a LVD cleanly punched the witness plate when exceeding 3.2 mm/μs. Significantly deeper dents from PBXN-109 filled with Dyno Nobel RS-RDX and RO Type I RDX did not occur until shock pressure was increased by a factor of two beyond the reaction threshold. In instrumented ELSGTs on the Dyno Nobel RS-RDX fill, this second threshold corresponded to an accelerating front near the witness end of the acceptor, with the onset of detonation moving closer towards the gap for greater input pressures. It is speculated that a small fraction of the RDX reacts with the sensitivity of a Type II RDX but that the bulk does not react until shock pressures are doubled. Some very large crystals in RO Type I RDX, as will be discussed, could preferentially react to sustain LVD. This is similar to the mechanism for LVD in liquid explosives, where a weak front is sustained by reaction at collapsing voids near the inner wall of the confinement, those voids being created by cavitation from a precursor shock in the confinement. LVD has not been reported in solid explosives, but there are occasionally unusual gap test data that could be explained by LVD.

Many explanations for differences in the shock sensitivity of nitramine crystals have been proposed, with internal defects being recognized early. Green and James[12] reported that the increased shock sensitivity of Holston relative to Bridgwater HMX correlates with internal flaws and irregular surfaces seen by microscopy. Modern analytical techniques have correlated internal defect densities with sensitivity, one of the most recent being the comparison of neutron scattering measurements with LSGT sensitivity for some of the same RDX lots in this study.[13] Particle size and shape are also important, with smaller and more spherical particles with a narrow size distribution being less sensitive.[14,15] These explanations for differences in shock sensitivity are inadequate for the current results.

Sensitivity data from Tables III and V as well as from another PBXN-109 study[16] with four lots of Holston RDX (produced prior to the transfer of that facility to OSI) are shown in Figure 27 versus δ_{mean}. The wide range of LSGT P_i for PBXN-109 filled with Holston RDX is not atypical and spans that for the other sources of RDX, including those with reduced sensitivity. LSGT thresholds increase with the δ_{mean} (approximated by solid line in Figure 27), whereas IMADGT and ELSGT thresholds are independent of δ_{mean} (shown by dashed line) except for HVD in the two less sensitive fills with RO Type I RDX and Dyno Noble RS-RDX. LVD for these two fills, however, has a similar threshold as HVD in the other fills. This observation is not necessarily in contrast with the reduced sensitivity of smaller particles when there is a relatively narrow size distribution. Larger δ_{mean} is actually a wider distribution of sizes within Class 1 RDX[1], as shown in Figure 28, which may improve crystal packing efficiency. Crystals as large as 2 mm were observed when trimming the end of IMADGT acceptors filled with RO Type I RDX. If improved packing efficiency reduced LSGT sensitivity, that benefit did not occur for the longer shock pulse from the ELSGT donor. This suggests that the LSGT thresholds are affected by d_c as well as shock sensitivity.

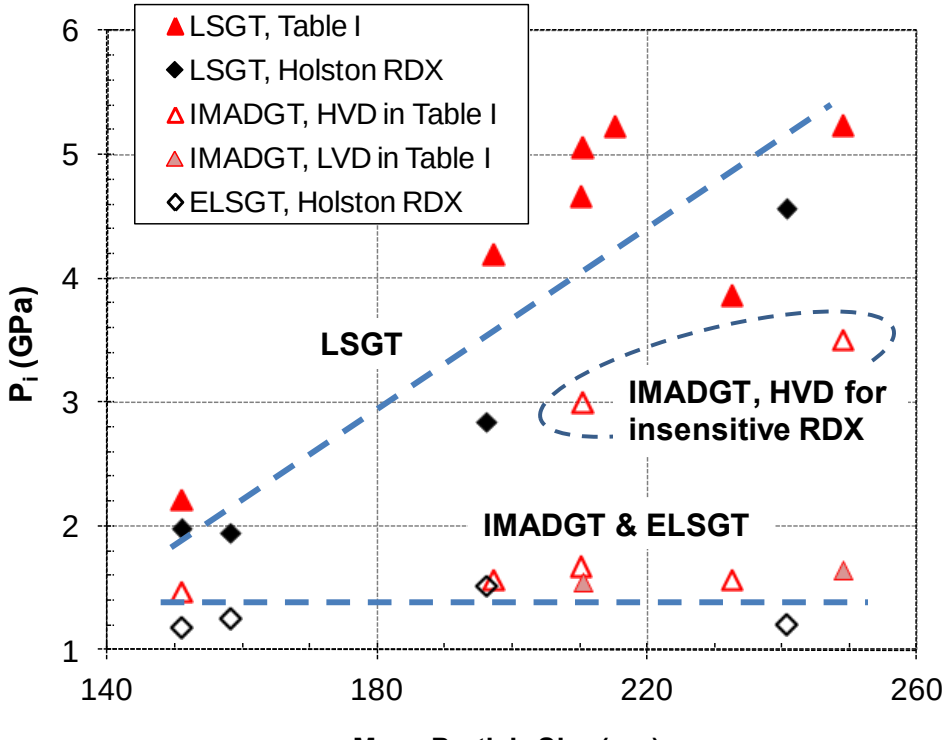

sts

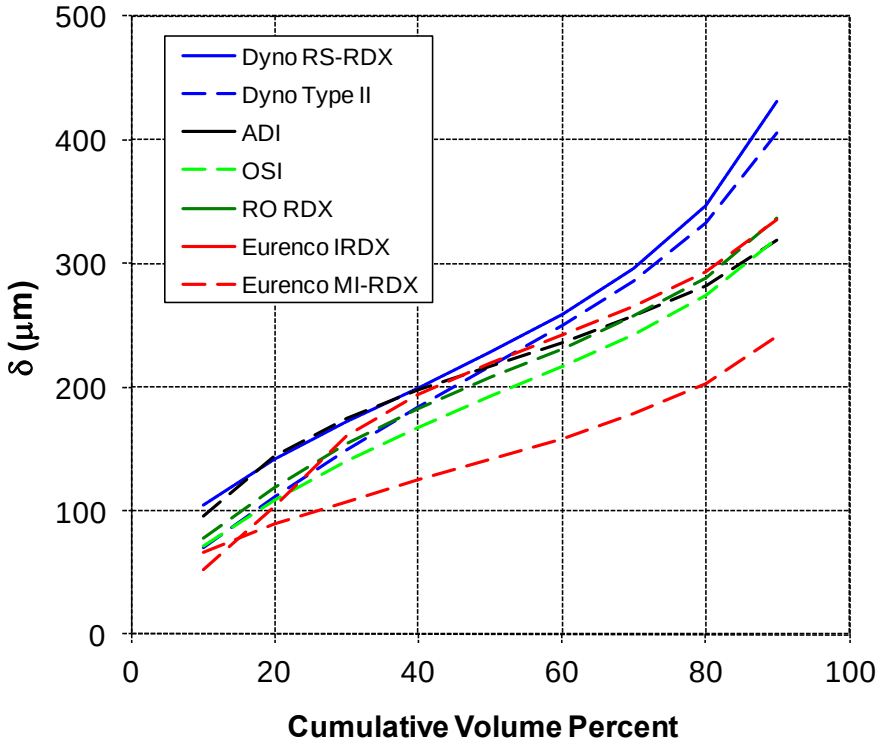

Figure 28. Particle Size Distribution for Various Lots of RDX

The decrease in diameter of the donor shock in the gap by lateral rarefactions[9] is illustrated in Figure 29. The first rarefaction in a LSGT gap reaches the axis in 34 mm, with P_G = 4.6 GPa. A second boundary is shown for an effective diameter where lateral rarefactions have reduced the shock pressure to 0.707 of that on axis. Lateral rarefactions continue to reduce shock diameter during run to detonation in the sample. If that shock diameter is less than d_c before shock growth in the sample begins to dominate, P_i needs to be higher than for a shock of larger diameter.

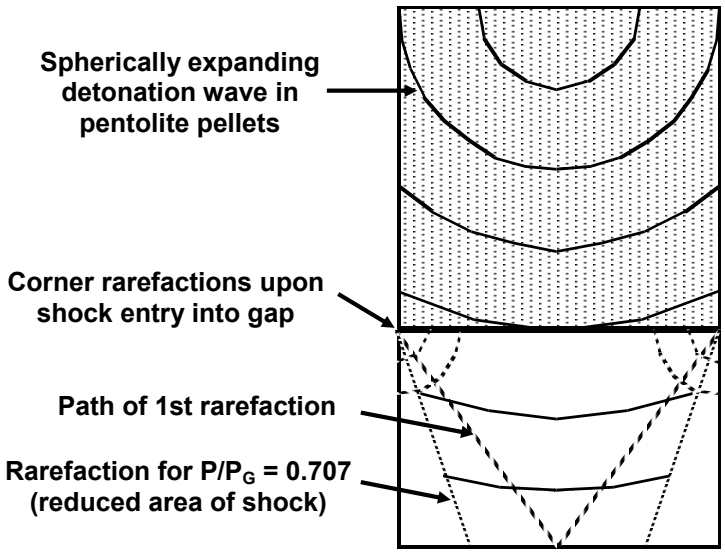

Figure 29. Reduction of Shock Diameter in Gap Test Donor by Lateral Rarefactions

In the IMAGT, the distinct onset of witness block dent depths >5 mm associated with the threshold of shock reaction is not that different than the ~8 mm deep dents associated with SDT in the ELSGT. This especially applies to fills with typical RDX sensitivity, whereas that ~3 mm difference in dent depth was significant for insensitive fills that did not exhibit rapid growth of shock reaction. The IMADGT shock reaction threshold may be the critical pressure for SDT at larger diameters, such as in the super large scale gap test. This could be important for sympathetic detonation from a large donor; whereas initiation by fragment attack would depend more on shock reaction at the smaller diameter of the LSGT.

A ~8-mm deep dent for the SDT threshold in PBXN-109 is essentially half of the maximum dent, which is a reasonable criterion for other explosives. This criterion is consistent with the IHE gap test.

Small-scale tests were performed[17] on samples from the same PBXN-109 mixes in this study with Dyno Nobel RS-RDX and Type II RDX. This arrangement uses a RISI RP-80 detonator with 203-mg of PETN as the donor and has a highly confined sample with a diameter of 7.24-mm, one fifth the size of an LSGT acceptor. Differences in sensitivity persisted, although with higher P_i to maintain constant energy fluence ($P_i^2\tau$, where τ is the shock duration) for the LSGT.

The effect of aging on IMADGT data depended upon the manufacturer, with no change in the Dyno Nobel RDXs, small changes in the Eurenco RDXs, a change in RO RDX from an insensitive fill to one of typical sensitivity, and a significant increase in sensitivity for the OSI Type II fill. These changes do not correlate with any difference in small-scale safety data but are consistent with the browning of RO Type I RDX and Holston Type II RDX crystals in aged samples, and the absence of browning in Eurenco MI-RDX crystals. This browning phenomenon is not yet understood and will be further studied.

There was sometimes (Figures 22-24) variability or an anomalous response in dent depth near the onset of shock reaction. While there are small variations in the castings, this could be related to delayed reaction of the explosive after it is propelled across the 12.7-mm air gap and impacts the witness block. Limited studies on other energetic materials exhibited consistent data near the reaction threshold when using an IMADGT arrangement without the air gap at the witness. Some gap test arrangements, dating back to the LSGT in the 1950s, include an air gap at the witness to prevent the witness plate from shattering and thereby facilitate interpretation of test results.[6] The air gap also eliminates reflection of a strong shock back into the acceptor and possibly avoids a false initiation; but this rationale is undocumented and double shocks are not very effective initiators.

SUMMARY AND CONCLUSIONS

The IMADGT provides a continuous measure of shock reaction as a function of P_G instead of just the threshold for punching a witness plate in other gap tests. There was a threshold of sustained shock reaction in PBXN-109 that was essentially independent of the RDX fill. Just beyond that threshold there was the rapid growth of reaction required for SDT in fills of Type II RDX sensitivity. That rapid growth of reaction was delayed until much higher pressures in fills with reduced sensitivity RDX. Gap pressures resulting in an 8-mm deep dent (half of the maximum) correlated with P_i in the ELSGT. At even higher shock pressures, IMADGT dent depths were consistent, suggesting a threshold for prompt shock reaction that is also independent of the RDX fill.

IMADGT data for insensitive RDX fills revealed an unusual shock reaction mechanism that manifested itself as LVD in LSGT and ELSGT acceptors. It is speculated that a small fraction of the RDX reacts with the sensitivity of a Type II RDX but that the bulk does not react until shock pressures are doubled. These differences in shock reaction were determined in the IMADGT without the instrumentation required for the LSGT and ELSGT, which also would benefit from a dent block instead of the currently used witness plate to distinguish between LVD and HVD. Furthermore, the IMADGT requires only 36% of the sample needed for the ELSGT, which is advantageous as a new ingredient is being developed or if the firing site has limitations. In this study, the reduced sample requirements of the IMADGT allowed additional acceptors for thirteen months of aging at 70^{o}C. The aged samples illustrated long term advantages of Dyno Nobel RS-RDX, a loss of insensitivity in RO RDX, and increased sensitivity for OSI RDX. The RDX crystals from RO and OSI had browned with aging, requiring further study.

REFERENCES

1. Thomasson, J. N., III, NSWC, Indian Head Division, private communication.
2. Doherty, R. M. and Watt, D. S., "Relationship Between RDX Properties and Sensitivity," *Propellants, Explosives, Pyrotechnics*, Vol. 33, No. 1, 2008, pp. 4-13.
3. Sandusky, H. W., Felts, J. E., Granholm, R. H., and Doherty, R. M., "Gap Test Phenomena – PBXN-109 Data For Different RDX Fills and Arrangements," 24th JANNAF Propulsion Systems Hazards Subcommittee (PSHS) Meeting, JSC CD-53, Chemical Propulsion Information Analysis Center, May 2008.
4. Sandusky, H. W., Felts, J. E., Granholm, R. H., "Shock Reaction of Two Different RDX Fills in PBXN-109," Shock Compression of Condensed Matter – 2009, AIP Conf. Proc. 1195, Part 1, pp. 237-240, 2009.
5. Sandusky, H. W. and Clark, K. A., "Effects of Aging on Shock Reaction of PBXN-109 with Different RDX Fills," 25th JANNAF PSHS Meeting, JSC CD-60, Dec 2009.
6. Price, D., Clairmont, A. R., Jr., and Erkman, J. O., "The NOL Large Scale Gap Test. III. Compilation of Unclassified Data and Supplementary Information for Interpretation of Results," NOLTR 74-40, Naval Ordnance Laboratory, White Oak, MD, 8 Mar 1974.
7. Liddiard, T. P. and Price, D., "The Expanded Large Scale Gap Test," NSWC TR 86-32, Naval Surface Warfare Center, White Oak, MD, Mar 1987.
8. Bernecker, R. R., "Concerning the Standardization of Gap Tests," in Proceedings of 1990 JANNAF Propulsion Systems Hazards Subcommittee Meeting, CPIA Publ. 538, Vol. I, 1990, pp. 187-195.
9. Sandusky, H. W., "Review of Gap Tests," Proceedings of 20th JANNAF Propulsion Systems Hazards Subcommittee Meeting, CPIA Publication 714, Vol. I, April 2002, pp. 283-296.
10. Department of Defense Ammunition and Explosives Hazard Classification Procedures, TB 700-2/ NAVSEAINST 8020.8B/TO 11A-1-47/DLAR 8220.1, 5 Jan 1998.
11. Sutherland, G. T., "Modeling of Large Scale and Expanded Large Scale Gap Test using the CTH Hydrocode," Proceedings of 14th International Detonation Symposium, ONR-351-10-185, Office of Naval Research, pp. 685-694, 2010.
12. Green, L. G. and James, E., Jr., "Radius of Curvature Effect on Detonation Velocity," Proceedings of Fourth Symposium (International) on Detonation," ACR-126, Office of Naval Research, pp. 86-91, 1965.
13. Stoltz, C. A., Hooper, J. P., Mason, B. P., and Roberts, C. W., "Small Angle Neutron Scattering Studies of RDX Defect Structure," Proceedings of 14th International Detonation Symposium, ONR-351-10-185, Office of Naval Research, pp. 1106-1112, 2010.
14. Moulard, H., "Particular Aspect of the Explosive Particle Size Effect on Shock Sensitivity of Cast PBX Formulations," Ninth Symposium (International) on Detonation, OCNR 113291-7, Office of the Chief of Naval Research, Vol. I, pp. 18-24, 1989.
15. van der Steen, A. C., Verbeek, H. J., and Meulenbrugge, J. J., "Influence of RDX Crystal Shape on the Shock Sensitivity of PBXs," Ninth Symposium (International) on Detonation, OCNR 113291-7, Office of the Chief of Naval Research, Vol. I, pp 83-88, 1989.
16. Davie, L., NSWC, Indian Head Division, private communication.
17. Felts, J. E., Sandusky, H. W., and Granholm, R. H., "Small-Scale Testing For Development of Explosives," Proceedings of 14th International Detonation Symposium, ONR-351-10-185, Office of Naval Research, pp. 664-674, 2010.

APPENDIX A:

IMADGT Data

Table A1. IMADGT Data for PBXN-109 Filled with Dyno Nobel RS-RDX

Mix No.	Test Date & Location	Gap (in)	Gap (mm)	P_G (GPa)	Dent (in)	Dent (mm)
307	9/26/05 @ Fort A.P. Hill	0.100	2.54	16.45	0.6655	16.90
		2.000	50.80	5.20	0.615	15.62
		2.250	57.15	4.74	0.5575	14.16
		2.522	64.06	4.21	0.541	13.74
		2.622	66.60	3.89	0.5285	13.42
		2.693	68.40	3.69	0.4328	10.99
		2.759	70.08	3.51	0.324	8.23
		2.835	72.01	3.31	0.289	7.34
		3.002	76.25	2.93	0.2993	7.60
		3.363	85.42	2.27	0.2818	7.16
		3.759	95.48	1.77	0.2393	6.08
		4.509	114.53	1.21	0.001	0.03
	8/07 @ IH bombproof	3.497	88.82	2.08	0.251	6.38
		3.9975	101.54	1.56	0.005	0.13
		4.119	104.62	1.46	0.000	0.00
		4.317	109.65	1.32	0.002	0.05
225	7/08 @ Fort A.P. Hill	3.200	81.28	2.54	0.285	7.24
		2.800	71.12	3.40	0.313	7.95
		3.801	96.55	1.73	0.237	6.02
		3.900	99.06	1.64	0.231	5.87
307, Aged Samples	8/09 @ Fort A.P. Hill	5.006	127.2	0.96	0.231	5.87
		5.020	127.5	0.96	0.013	0.33
		5.055	128.4	0.94	0.020	0.51
		5.108	129.7	0.92	0.013	0.33
		5.205	132.2	0.88	0.003	0.08

Table A2. IMADGT Data for PBXN-109 Filled with Dyno Nobel Type II RDX

Mix No.	Test Date & Location	Gap (in)	Gap (mm)	P_G (GPa)	Dent (in)	Dent (mm)
308	9/30/05 @ Fort A.P. Hill	0.102	2.59	16.38	0.658	16.71
		2.000	50.80	5.20	0.597	15.16
		2.545	64.64	4.14	0.601	15.27
		2.744	69.70	3.55	0.593	15.06
		3.000	76.20	2.93	0.557	14.15
		3.245	82.42	2.46	0.513	13.03
		3.374	85.70	2.25	0.522	13.26
		3.496	88.80	2.08	0.469	11.91
		3.740	95.00	1.79	0.423	10.74
		3.999	101.57	1.56	0.270	6.86
		4.250	107.95	1.37	0.258	6.55
		4.500	114.30	1.21	0.001	0.03
	8/07 @ IH bombproof	4.313	109.55	1.33	0.025	0.64
		4.398	111.71	1.27	0.208	5.28
226	7/08 @ Fort A.P. Hill	3.802	96.571	1.73	0.258	6.55
		4.002	101.65	1.55	0.231	5.87
		4.106	104.29	1.47	0.124	3.15
		4.399	111.73	1.27	0.000	0.00
308, Aged Samples	8/09 @ Fort A.P. Hill	3.203	81.36	2.54	0.512	13.00
		3.753	95.33	1.78	0.433	11.00
		4.001	101.63	1.55	0.332	8.43
		4.253	108.03	1.37	0.070	1.78
		4.352	110.54	1.30	0.185	4.70
		4.502	114.35	1.21	0.002	0.05
		4.505	114.43	1.21	0.002	0.05

Table A3. IMADGT Data for PBXN-109 Filled with Eurenco I-RDX

Mix No.	Test Date & Location	Gap (in)	Gap (mm)	P_G (GPa)	Dent (in)	Dent (mm)
302	9/22/05 @ Fort A.P. Hill	0.100	2.54	16.45	0.686	17.42
		2.470	62.74	4.37	0.580	14.73
		2.740	69.60	3.56	0.568	14.43
		2.835	72.01	3.31	0.544	13.82
		3.004	76.30	2.92	0.450	11.43
		3.147	79.93	2.64	0.437	11.10
		3.361	85.37	2.27	0.407	10.34
		3.764	95.61	1.77	0.370	9.40
		4.135	105.03	1.45	0.229	5.82
		4.307	109.40	1.33	0.261	6.63
		4.505	114.43	1.21	0.001	0.03
		6.000	152.40	0.66	0.001	0.03
	8/07 @ IH bombproof	3.498	88.85	2.08	0.409	10.39
		3.997	101.52	1.56	0.373	9.47
		4.148	105.36	1.44	0.302	7.67
302, Aged Samples	8/09 @ Fort A.P. Hill	2.800	71.12	3.40	0.552	14.02
		3.403	86.44	2.21	0.481	12.22
		4.200	106.68	1.40	0.346	8.79
		4.397	111.68	1.27	0.167	4.24
		4.608	117.04	1.15	0.385	9.78
		4.803	122.00	1.05	0.000	0.00

Table A4. IMADGT Data for PBXN-109 Filled with Eurenco MI-RDX

Mix No.	Test Date & Location	Gap (in)	Gap (mm)	P_G (GPa)	Dent (in)	Dent (mm)
301	9/30/05 @ Fort A.P. Hill	0.096	2.44	16.6	0.647	16.43
		2.508	63.70	4.26	0.589	14.96
		2.996	76.10	2.94	0.552	14.02
		3.254	82.65	2.45	0.539	13.69
		3.501	88.93	2.07	0.455	11.56
		3.635	92.33	1.91	0.537	13.64
		3.769	95.73	1.76	0.509	12.93
		3.925	99.70	1.62	0.507	12.88
		4.000	101.60	1.55	0.455	11.56
		4.127	104.83	1.46	0.308	7.82
		4.256	108.10	1.36	0.241	6.12
		4.505	114.43	1.21	0.001	0.03
301, Aged Samples	8/09 @ Fort A.P. Hill	3.902	99.11	1.64	0.517	13.13
		4.201	106.71	1.40	0.474	12.04
		4.405	111.89	1.27	0.344	8.74
		4.508	114.50	1.21	0.131	3.33
		4.603	116.92	1.15	0.185	4.70
		4.653	118.19	1.13	0.001	0.03
		4.703	119.46	1.10	0.000	0.00
		4.755	120.78	1.08	0.001	0.03

Table A5. IMADGT Data for PBXN-109 Filled with Holston RDX

Mix No.	Test Date & Location	Gap (in)	Gap (mm)	P_G (GPa)	Dent (in)	Dent (mm)
306	9/21/05 @ Fort A.P. Hill	0.100	2.5	16.45	0.639	16.23
		2.486	63.1	4.33	0.566	14.38
		3.000	76.2	2.93	0.527	13.39
		3.159	80.2	2.62	0.546	13.87
		3.266	83.0	2.43	0.506	12.85
		3.378	85.8	2.25	0.468	11.89
		3.758	95.5	1.77	0.412	10.46
		4.125	104.8	1.46	0.278	7.06
		4.325	109.9	1.32	0.198	5.03
		4.421	112.3	1.26	0.003	0.08
		4.500	114.3	1.21	0.006	0.15
		6.000	152.4	0.66	0.001	0.03
306, Aged Samples	8/09 @ Fort A.P. Hill	4.007	101.8	1.55	0.504	12.80
		4.508	114.5	1.21	0.426	10.82
		4.901	124.5	1.01	0.260	6.60
		5.006	127.2	0.96	0.231	5.87
		5.020	127.5	0.96	0.013	0.33
		5.055	128.4	0.94	0.020	0.51
		5.108	129.7	0.92	0.013	0.33
		5.205	132.2	0.88	0.003	0.08

Table A6. IMADGT Data for PBXN-109 Filled with Royal Ordnance RDX

Mix No.	Test Date & Location	Gap (in)	Gap (mm)	P_G (GPa)	Dent (in)	Dent (mm)
300	9/27/05 @ Fort A.P. Hill	0.105	2.67	16.27	0.639	16.23
		2.000	50.80	5.20	0.584	14.83
		2.256	57.30	4.73	0.601	15.27
		2.509	63.73	4.25	0.573	14.55
		2.600	66.04	3.96	0.554	14.07
		2.750	69.85	3.53	0.569	14.45
		2.785	70.74	3.44	0.499	12.67
		2.800	71.12	3.40	0.424	10.77
		2.868	72.85	3.23	0.382	9.70
		3.000	76.20	2.93	0.311	7.90
		3.256	82.70	2.44	0.307	7.80
		4.499	114.27	1.21	0.001	0.03
	8/07 @ IH bombproof	3.499	88.86	2.08	0.298	7.57
		3.753	95.31	1.78	0.262	6.65
		4.002	101.64	1.55	0.209	5.31
		4.331	110.01	1.31	0.000	0.00
308, Aged Samples	8/09 @ Fort A.P. Hill	3.352	85.14	2.29	0.435	11.05
		3.825	97.16	1.71	0.396	10.06
		4.198	106.63	1.40	0.225	5.72
		4.401	111.79	1.27	0.029	0.74

DISTRIBUTION

OUSD(AT&L)/PSA/LW&M
ATTN DD LAND WARFARE AND MUNITIONS
3090 DEFENSE PENTAGON ROOM 5C756
WASHINGTON DC 20301-3090 1 CD

NAVAL AIR WARFARE CENTER
ATTN 474000D (D HILL)
1 ADMINISTRATIVE CIRCLE
MAIL STOP 1109
CHINA LAKE CA 93555-6001 1 CD

NAVAL AIR WARFARE CENTER
ATTN 474200D (A ATWOOD)
1 ADMINISTRATIVE CIRCLE
MAIL STOP 1109
CHINA LAKE CA 93555-6001 1 CD

NAVAL AIR WARFARE CENTER
ATTN 474100D (M MASON)
2400 E PILOT PLANT ROAD
MAIL STOP 5202
CHINA LAKE CA 93555-6107 1 CD

NAVAL AIR WARFARE CENTER
ATTN 474100D (A NELSON)
2400 E PILOT PLANT ROAD
MAIL STOP 5202
CHINA LAKE CA 93555-6107 1 CD

NAVAL AIR WARFARE CENTER
ATTN 474100D (Q BUIDANG)
2400 E PILOT PLANT ROAD
MAIL STOP 5202
CHINA LAKE CA 93555-6107 1 CD

NAVAL AIR WARFARE CENTER
ATTN 47J270D (B BURCHETT)
2400 E PILOT PLANT ROAD
MAIL STOP 6811
CHINA LAKE CA 93555-6107 1 CD

NAVAL AIR WARFARE CENTER
ATTN 47J270D (B WEICH)
2400 E PILOT PLANT ROAD
MAIL STOP 6811
CHINA LAKE CA 93555-6107 1 CD

NAVAL AIR WARFARE CENTER
ATTN 478200D (J DUCHOW)
2400 E PILOT PLANT ROAD
MAIL STOP 5402
CHINA LAKE CA 93555-6107 1 CD

NAVAL AIR WARFARE CENTER
ATTN 478300D (J KANDELL)
2400 E PILOT PLANT ROAD
MAIL STOP 5403
CHINA LAKE CA 93555-6107 1 CD

OFFICE OF NAVAL RESEARCH
ATTN GIL GRAFF
ONE LIBERTY CENTER
875 NORTH RANDOLPH STREET
SUITE 351
ARLINGTON VA 22203 1 CD

OFFICE OF NAVAL RESEARCH
ATTN CLIFFORD BEDFORD
ONE LIBERTY CENTER
875 NORTH RANDOLPH STREET
SUITE 351
ARLINGTON VA 22203 1 CD

OFFICE OF NAVAL RESEARCH
ATTN MATT BEYARD, CODE 33
ONE LIBERTY CENTER
875 NORTH RANDOLPH STREET
ROOM 602B
ARLINGTON VA 22203 1, 1 CD

NAVAL ORDNANCE SAFETY & SECURITY ACTIVITY
ATTN KERRY CLARK, FARRAGUT HALL
3817 STRAUSS AVE SUITE 108
INDIAN HEAD MD 20640-5151 1 CD

RUTH DOHERTY
12604 LAURIE DRIVE
SILVER SPRING MD 20904 1, 1 CD

AFRL/RWME
ATTN STEPHEN STRUCK
2306 PERIMETER ROAD
EGLIN AFB, FL 32542 1, 1 CD

AFRL/RWME
ATTN THOMAS KRAWIETZ
2306 PERIMETER ROAD
EGLIN AFB, FL 32542 1, 1 CD

Internal:

ALBERT T CAMP TECHNICAL LIBRARY
4171 FOWLER ROAD SUITE 103
INDIAN HEAD, MD 20640-5110

ORDNANCE ASSESSMENT DIVISION IHDIV NSWC
ATTN BRUCE THOMAS, BLDG 302
4103 FOWLER ROAD, SUITE 117
INDIAN HEAD MD 20640-5106 1 CD

RESEARCH & TECH DIV IHDIV NSWC
ATTN HAROLD SANDUSKY, BLDG 600
4104 EVANS WAY SUITE 102
INDIAN HEAD MD 20640-5102 1, 1 CD

RESEARCH & TECH DIV IHDIV NSWC
ATTN RICHARD LEE, BLDG 600
4104 EVANS WAY SUITE 102
INDIAN HEAD MD 20640-5102 1 CD

RESEARCH & TECH DIV IHDIV NSWC
ATTN RICHARD GRANHOLM, BLDG 600
4104 EVANS WAY SUITE 102
INDIAN HEAD MD 20640-5102 1

RESEARCH & TECH DIV IHDIV NSWC
ATTN JOSHUA FELTS, BLDG 600
4104 EVANS WAY SUITE 102
INDIAN HEAD MD 20640-5102 1 CD

RESEARCH & TECH DIV IHDIV NSWC
ATTN LORI NOCK, BLDG 302
4103 FOWLER ROAD SUITE 107
INDIAN HEAD MD 20640-5107 1 CD

RESEARCH & TECH DIV IHDIV NSWC
ATTN MARY SHERLOCK, BLDG 302
4103 FOWLER ROAD SUITE 107
INDIAN HEAD MD 20640-5107 1 CD

RESEARCH & TECH DIV IHDIV NSWC
ATTN JOSEPH CHANG, BLDG 600
4104 EVANS WAY SUITE 102
INDIAN HEAD MD 20640-5102 1 CD

ENERGETIC TECHNOLOGY DIV IHDIV NSWC
ATTN ROBERT HUTCHESON, BLDG 302-114
4103 FOWLER ROAD SUITE 107
INDIAN HEAD MD 20640-5107 1 CD

Electronic Copy:

ADMINISTRATOR
DEFENSE TECH INFORMATION CTR
ATTN JACK RIKE OCA
8725 JOHN J KINGMAN RD STE 0944
FT BELVOIR VA 22060-6218

This page intentionally left blank.